



Investigating the response of LAI to droughts in southern African vegetation using observations and model-simulations.

Shakirudeen Lawal¹ Stephen Sitch² Danica Lombardozzi³ Julia E.M.S. Nabel⁴ Hao-Wei Wey⁴ Pierre Friedlingstein⁵ Hanqin Tian⁶ Bruce Hewitson¹

5 ¹Climate System Analysis Group, Department of Environmental and Geographical Science, University of Cape Town, Cape Town, 7700, South Africa

²College of Life and Environmental Sciences, University of Exeter, Exeter EX4 4QE, UK

10 ³National Center for Atmospheric Research, Climate and Global Dynamics, Terrestrial Sciences Section, Boulder, CO 80305, USA

⁴Max Planck Institute for Meteorology, Hamburg, Germany

⁵College of Engineering, Mathematics and Physical Sciences, University of Exeter, Exeter EX4 4QF, UK

15 ⁶School of Forestry and Wildlife Sciences, Auburn University, 602 Duncan Drive, Auburn, AL 36849, USA

*Corresponding author: lasd_dr@yahoo.com

20

25



30 Abstract

In many regions of the world, frequent and continual dry spells are exacerbating drought conditions, which have severe impacts on vegetation biomes. Vegetation in southern Africa is among the most affected by drought. Here, we assessed the spatiotemporal characteristics of meteorological drought in southern Africa using the Standardized Precipitation Evapotranspiration Index over a 30-year period (1982 – 2011). The severity and the effects of droughts on vegetation productiveness were examined at different drought time-scales (1- to 24-month time-scales). In this study, we characterized vegetation using the Leaf Area Index, after evaluating its relationship with the Normalized Difference Vegetation Index. We found that the LAI responds strongly ($r = 0.6$) to drought over the central and south eastern parts of the region, with weaker impacts ($r < 0.4$) over parts of Madagascar, Angola and western parts of South Africa. Furthermore, the latitudinal distribution of LAI responses to drought indicates a similar temporal pattern but different magnitudes across timescales. The results of the study also showed that the seasonal response across different southern African biomes varies in magnitude and occurs mostly at shorter to intermediate timescales. The semi-desert biome strongly correlates ($r = 0.95$) to drought at 6-month timescale in the MAM (summer) season, while the tropical forest biome shows the weakest response ($r = 0.35$) at 6-month timescale in the DJF (hot and rainy) season. In addition, we found a stronger response (in the year 1983, $r = 0.84$ over Namibia and eastern parts of South African) of the LAI to drought during dry years as compared to wet years; and we found different temporal variability in global and regional responses across different biomes.

We also examined how well an ensemble of state of the art dynamic global vegetation models (DGVMs) simulate the LAI and its response to drought. The spatial and seasonal response of the LAI to drought is mostly overestimated in the DGVM multi-model ensemble compared to the observations. The correlation coefficient values for the multi-model ensemble are as high as 0.76 (annual) over South Africa, and 0.98 in MAM season over the temperate grassland biome. Furthermore, the DGVM model ensemble shows positive biases (3-month or longer) in the simulation of spatial distribution of drought timescales and overestimate the seasonal distribution timescales. The results of this study may highlight areas to target for further development of DGVMs in order to improve the models' capability in simulating the drought-vegetation relationship.

60 **Keywords:** Drought intensity; Drought indices; Standardized precipitation evapotranspiration index; DGVMs; southern Africa; Drylands



1 Introduction

70 Drought can be described as a natural occurrence whereby the natural accessibility of water for a region is beneath the normal state over a long period of time (Xu *et al.*, 2015). Globally, it is considered one of the world's most important climate risks, with significant environmental, social and ecological impacts on different sectors (e.g. agriculture, forestry, hydrology) and human lives (Naumann *et al.*, 2018). Increasing trends in the occurrence and severity of drought in West Africa and Mediterranean have huge impacts on water resources and agriculture (Sultan and Gaetani, 75 2016). In southern Africa, a region regarded as a climate hotspot because of the projected impacts of climate change on its numerous endemic vegetation, an understanding of these impacts is important for mitigation options in managing future drought events. Therefore, it is important to examine drought impacts on vegetation and evaluate how this is simulated in models.

Drought is a frequent occurrence in southern Africa, and has enormous impacts on vegetation in 80 the region. For instance, drought has resulted in a significant loss of biomes and death of plants (Masih, 2007, Hoffman *et al.*, 2009). It is reported that there are now fewer vegetation coverage in the region compared to what existed between the mid 1990's and 2000's (EOS, 2007). Furthermore, there are projections that by mid-century, southern Africa may lose about one-third of its current vegetation due to increasing exacerbation of drought in the region (Scott, 2005). 85 Drought has also impacted speciation of vegetation thereby causing significant changes to the region's rich biomes, through the lack of formation of new species or even growth of species with underdeveloped morphological and physiological characteristics (Hoffman *et al.*, 2009). Drought-induced vegetation loss has both ecological and socio-economic consequences on human lives. For instance, studies have shown that food security in the region is threatened due to the continual 90 mortality of vegetation (FAO, 2000; Muller, 2003). Other studies (e.g. Wang, 2010; Khosravi, 2017) have also reported that southern Africa could lose more than \$200 billion of its GDP from the effects of drought on vegetation. The enormous impacts on vegetation have thus made it imperative to investigate how vegetation might respond to different drought intensities at varying timescales.

95 In order to monitor and quantify drought characteristics, drought indices are used (Wilhite and Glantz, 1985). Drought indices including the SPI (i.e. the standardized precipitation index), standardized water-level index and standardized anomaly index are derived from a single hydrological variable i.e. rainfall (Kwon *et al.*, 2019). Other indices such as the Palmer drought severity index, multivariate standardized drought index and standardized precipitation 100 evapotranspiration index (SPEI) combine two or more variables related to other atmospheric or soil and environmental conditions that may predispose a plant to water stress (Palmer, 1965; Vicente-Serrano *et al.*, 2010; Hao and AghaKouchak, 2013). Among the drought indices, the SPI is the most widely used because of the adjustable timescale and its relatively simple calculation (McKee *et al.*, 1993). It is also recognized as appropriate for use in southern Africa (Hoffman *et al.*, 2009). However, SPI has a significant shortcoming, which is that its computation uses only 105 rainfall without considering the effect of other meteorological variables in the development of drought occurrence (Teuling *et al.*, 2013). In order to address this shortcoming, SPEI was developed for drought monitoring and it is regarded as a more suitable drought index in the region to investigate the spatiotemporal scale of drought (Ujeneza and Abiodun, 2014). SPEI is computed 110 from the difference between potential evapotranspiration (PET) and rainfall (Vicente-Serrano *et al.*, 2010). PET can be computed using different methods such as Hargreaves (HG) and Penman-



Monteith (PM) method. Although studies (e.g. Vicente-Serrano *et al.*, 2010) have found that PM method captures drought better than HG, other studies (e.g. Lawal *et al.*, 2019) showed this difference is negligible over southern Africa.

115 Many studies have used different indices to quantify observed drought, characterize vegetation,
and study drought effects on the productiveness of vegetation across different timescales. Several
studies (e.g. Vicente-Serrano *et al.*, 2015; Zhang *et al.*, 2016; Lawal *et al.*, 2019a,b) have shown
that the satellite-derived normalized difference vegetation index (NDVI) is one the most important
120 indicators of vegetation health and greenness. These studies applied NDVI in examining drought
impacts on vegetation on global vegetation biomes. However, other studies (Gitelson, 2004;
Santin-Janin *et al.*, 2009) have argued that while NDVI is a true proxy for vegetation trends, its
potential saturation makes it difficult to fully estimate biomass. In addition, because the NDVI
parameters are not well calibrated and often missing in models, simulated NDVI can be biased.
Due to its high correlation with NDVI, the leaf area index (LAI) is instead used to characterize
125 vegetation conditions (Fan *et al.*, 2007; Zhao *et al.*, 2018). Although the LAI is an important
vegetation proxy, it is rarely considered in the estimation of drought impacts on vegetation. Thus,
quantifying the response of the LAI to drought over southern Africa is important for understanding
the processes that modulate ecosystem services produced by vegetation which are crucial for
human survival. (Melillo 2015).

130 Previous studies have also evaluated the performance of coupled climate models in simulating the
response of vegetation to drought. For instance, Lawal *et al.* (2019a) reported that an ensemble of
the Community Earth System Model (CESM) showed biases in response simulation of vegetation
to drought. This was attributed to the parameterizations of the land component (i.e. Community
Land Model, CLM) which poorly simulated observed NDVI. Given the poor replication of
135 vegetation response to drought by a coupled climate model, there is a need to examine land-only
models and whether they might better capture drought-vegetation relationship when the
atmospheric forcings are derived from observations. The present study used Dynamic Global
Vegetation models (DGVMs) to study vegetation response to drought, as little is known on how
the LAI response to drought is simulated by DGVMs. The choice of DGVMs is because of their
140 capability in simulating mostly accurate carbon exchange between atmosphere and vegetation
ecosystems (Lu *et al.*, 2011).

The aim of this study is to investigate the response of LAI to droughts in southern African
vegetation using observations. We also examined how well the responses are represented in model
simulations. We used satellite and simulated LAI to quantify vegetation responses to drought. We
145 characterized the spatiotemporal extent of drought and its severity using the SPEI and then
assessed the influence of drought using the LAI from satellite data and model simulations.

2 Data and Methodology

2.1 Data

150 In this study, we used satellite and simulated LAI, and satellite NDVI; gridded observation and
reanalysis climate datasets. The gridded observation climate datasets included precipitation,
maximum, mean and minimum temperature. These data were gotten from CRU (i.e. the Climate



155 Research Unit; Mitchell & Jones, 2005; Harris *et al.*, 2014). These are global monthly data which
have $0.5^\circ \times 0.5^\circ$ as spatial resolution and spans 1901 – 2019 period. Here, we used the CRU data
for the period 1982 – 2011 to compute observed drought indices (i.e. SPEI) to characterize the
spatiotemporal severity of drought. CRU is a gridded observed datasets, which was used because
of its suitable spatial and temporal resolutions. The reanalysis climate data we used are the
CRUJRA, which is a combination of CRU and the Japanese Reanalysis data (JRA) (University of
160 East Anglia Climatic Research Unit; Harris, I.C., 2019). It is a 6-hourly, land surface, gridded data
with a spatial resolution $0.5^\circ \times 0.5^\circ$. CRUJRA was used to compute reanalysis drought indices and
used for model simulations. Here we aggregated CRUJRA to monthly samples and used the data
at the same spatial and temporal resolution as CRU.

165 For the satellite vegetation indices, first, we used the third generation of NDVI (hereafter,
NDVI3g) from the Global Inventory Modelling and Mapping Studies (GIMMS), and spans period
from 1981 – 2015, temporal resolution of biweekly and a spatial resolution of about 8km (Pinzon
and Tucker, 2014; National Center for Atmospheric Research Climate Data Guide, accessed 2019).
Here, we used the data for the period 1982 – 2011. Furthermore, we used the third generation of
170 the GIMMS LAI (LAI3g) which also spans the period 1981 – 2015; has a temporal resolution of
biweekly and spatial resolution as GIMMS3g. The LAI data had been processed (at source) using
a set of neural networks which were first trained on highest-quality and post-processed MODIS
LAI and FPAR products and AVHRR GIMMS NDVI3g data for the overlapping period (2000 to
2009). The trained neural networks were then used to produce the LAI3g and FPAR3g data sets
(Mao and Yan, 2019). For the study, LAI3g was also used for the period 1982 – 2011.

175 The simulated monthly LAI data were obtained from eleven Dynamic Global Vegetation Models
(DGVMs) which are part of the Trendy-version 7 (Sitch *et al.*, 2008; Le Quéré *et al.*, 2018). These
DGVMs are CABLE-POP (Haverd *et al.*, 2018), CLM (Oleson *et al.*, 2013), CLASS-CTEM
(Melton and Arora, 2016), DLEM (Tian *et al.*; 2015), JSBACH (Mauritsen *et al.*, 2018), LPX
180 (Lienert and Joos; 2018), OCN (Zaehle and Friend; 2010), ORCHIDEE (Goll *et al.*, 2017),
SURFEX (Joezjtjer *et al.*, 2015), JULES (Clark *et al.*; 2011) and VISIT (Kato *et al.*, 2013). LAI
from the models have a monthly temporal resolution spanning period from 1901 – 2017. We
selected these DGVMs because they have been run with similar protocol (S3 simulations) and
forcing datasets (i.e. CRUJRA).

185

2.2 Methods overview

2.2.1 Evaluation of DGVMs and the relationship between NDVI and LAI

190 The relationship between NDVI and LAI was evaluated by computing the grid cell spatiotemporal
correlation between GIMMS NDVI and GIMMS LAI, as well as spatiotemporal correlation
between GIMMS LAI and simulated LAI from individual DGVMs. This was necessary to show
whether LAI is an appropriate estimator of NDVI, and how well the models simulate the LAI in
the region.

195 The climatology of observed and simulated climatic variables as well as LAI over six major biomes
in southern Africa for the period 1982- 2011 were computed. These biomes are semi desert,



Mediterranean, dry savanna, moist savanna, temperate grassland and tropical forest (Fig. 1; Sinclair & Beyers, 2015; Lawal *et al.*, 2019a, b).

200 2.2.2 Description of Drought

For the present study, we adopted the definition of meteorological drought, “which is described as a period (e.g. a season) during which there is a deficit in the magnitude of precipitation in a particular area compared to the long-term normal (Palmer, 1965; Wilhite & Glantz, 1985)”. Here, we used meteorological drought because it does not make any presumptions about soil characteristics or run-off. In addition, it is acknowledged to be a primary component in the depletion of vegetation productiveness and reduction of biomass (Vicente-Serrano, *et al.*, 2010). Previous studies (Vicente-Serrano *et al.*, 2006; Vicente-Serrano *et al.*, 2013) have also used meteorological drought in the investigation of drought impacts on biomass and vegetation productiveness. It is reported that there is a linkage in the attributes of meteorological and agricultural droughts which culminate in the deficit of soil moisture (Lake, 2011).

2.2.3 Drought computation and correlation with LAI

215 The analyses include calculating drought (i.e. SPEI) using CRU data over a 30-year (1982 – 2011) period for different drought timescales. The drought time-scale can be described as the aggregation of temporal duration (Vicente-Serrano *et al.*, 2010).

220 A time series of the evolution of drought for the 30-year period was plotted. The present study extends the timeframe for understanding drought impacts through 2011. The study goes to 2011 because there were droughts in the 2005 – 2011 window (Masih *et al.*, 2014). This extension is particularly important considering that southern Africa experiences more frequent droughts with impacts exacerbated by climate change. This information is important for considering adaptation measures and understanding the role of climate change.

225 The drought index, SPEI, is calculated from the deduction between precipitation (P) and potential evapotranspiration (PET) as shown below;

$$D = P - PET \dots\dots\dots (1)$$

230 where PET is computed from maximum temperature, minimum temperature and mean temperature, using Hargreaves technique (e.g. Vicente-Serrano *et al.*, 2012; Beguera *et al.*, 2014; Stagge *et al.*, 2014). D values are obtained through aggregation over individual time-scales which span 1- to 24-months (i.e. 1-, 3-, 6-, 9-, 12-, 15-, 18-, 21- and 24-month). The time-scales were calculated by including the variable past values effect. For example, a time-scale of 15-month suggest that input from the preceding 15 months, which includes the present month, was used for calculating SPEI (Beguera *et al.*, 2014). “For the 1-month timescale, only the current month data is used for the calculation. The D values were standardized by assuming a suitable statistical distribution (e.g. gamma, log-logistic). The log-logistic distribution was used to standardize the D values in this study”. For more details on the timescale computation, please see Vicente-Serrano *et al.* (2010); <https://rdr.io/cran/SPEI/man/spei.html>.



We note that the PET in the SPEI was computed using Hargreaves (HG) method rather than Penman-Montieth (PM) because the data (e.g. vapour pressure, maximum and minimum humidity) required for computing PM over southern Africa are sometimes missing or not available at the needed gridded spatial resolutions and timespan. Although PM is considered better in most regions, Lawal *et al.* (2019a) showed that the variation between the PM and HG is negligible for southern African region. The study only considered observed SPEI_PM which was obtained from <https://spei.csic.es/database.html> and not modelled SPEI_PM due to the unavailability of simulated data required for its computation. Other studies (e.g. Beguera *et al.*, 2014) have also found that there is an insignificant contrast in the strength of PM and HG for reproducing their divergence on measured variables such vegetation indexes.

We deseasonalized GIMMS LAI by transforming monthly LAI series per pixel to symbolize the standardized deviations from extended mean. This was to make the sequence of LAI commensurate to SPEI (Vicente-Serrano *et al.*, 2013) and eliminate the impact of periodicity on vegetation response. We note that SPEI is intrinsically deseasonalized.

We then computed the correlation per grid-cell between drought index (CRU) and deseasonalized LAI over the 30-year period at the different drought timescales using Pearson correlations. We then compared the spatial distribution of maximum (peak) correlation and the comparable time-scales of drought for observed SPEI.

Next, we investigated correlations at each grid cell between the drought (from reanalysis - CRUJRA) and an ensemble median of modelled LAI from individual DGVMs. The maximum (maximum) correlations and equivalent time-scales from the complete 1- to 24-month time-scales were mapped for the ensemble median over the 30-year period. We used ensemble median because of its less sensitivity to independent outliers (Reuter *et al.*, 2012). In summary, we calculated model ensemble drought from the indexes median from individual members' drought indexes. The inter-annual variation of drought impacts on LAI by individual DGVM was also calculated for different timescales.

In simple terms, CRU was used to compute observed drought while CRUJRA was used to calculate modeled drought because it is what was used to force the models. This will allow for easy observation and model comparisons

Similar to Lawal *et al.*, 2019a, we calculated the seasonal mean for four seasons i.e. a) December-January-February (DJF); b) March-April-May (MAM); c) June-July-August (JJA); and d) September-October-November (SON) from the correlations of monthly series of drought and LAI. These were computed from correlating monthly series (twelve series per year) per pixel of GIMMS-LAI and each monthly series of 1- to 24-months drought (SPEI) series over the 30-year period with Pearson correlation. The same technique was used for the model ensemble. We calculated the peak correlations and drought timescales of the models over six major biomes in southern Africa namely (Fig. 1) – Temperate grassland, Tropical forest, Moist Savanna, Dry Savanna, Semi-desert and Mediterranean vegetation. These regions were selected because of their relative importance and they are most affected by drought.



290 Finally, the impacts of extreme events (wet and dry years) at different time periods were compared;
and the comparison of global and regional responses to drought across biomes for the period 1982
– 2011 was investigated.

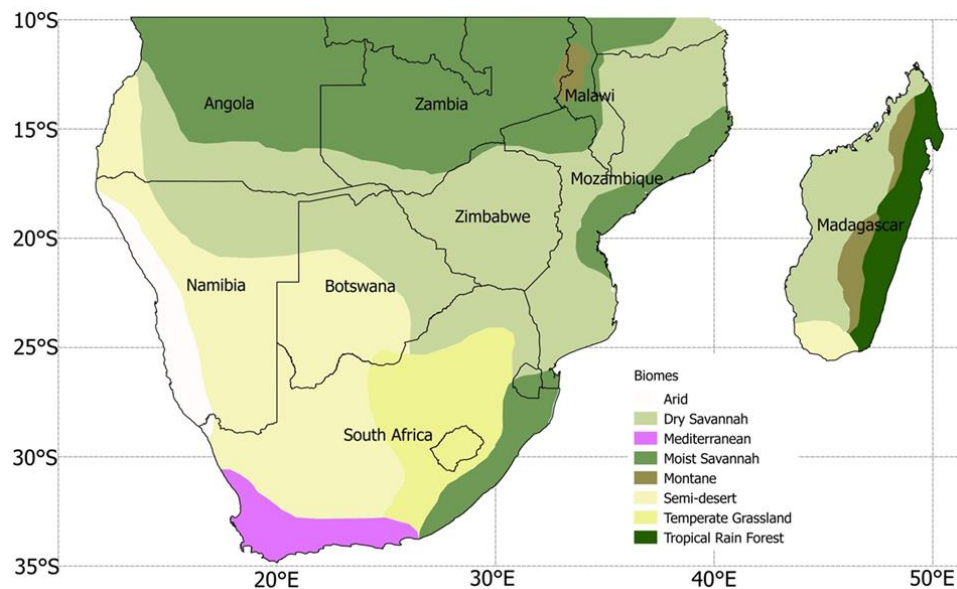


Figure 1. Major vegetation biomes in southern Africa (adapted from UNEP, 2008, Sinclair & Beyers, 2015 and Lawal *et al.*, 2019a,b). The black contours indicate political boundaries.

295

3 Results

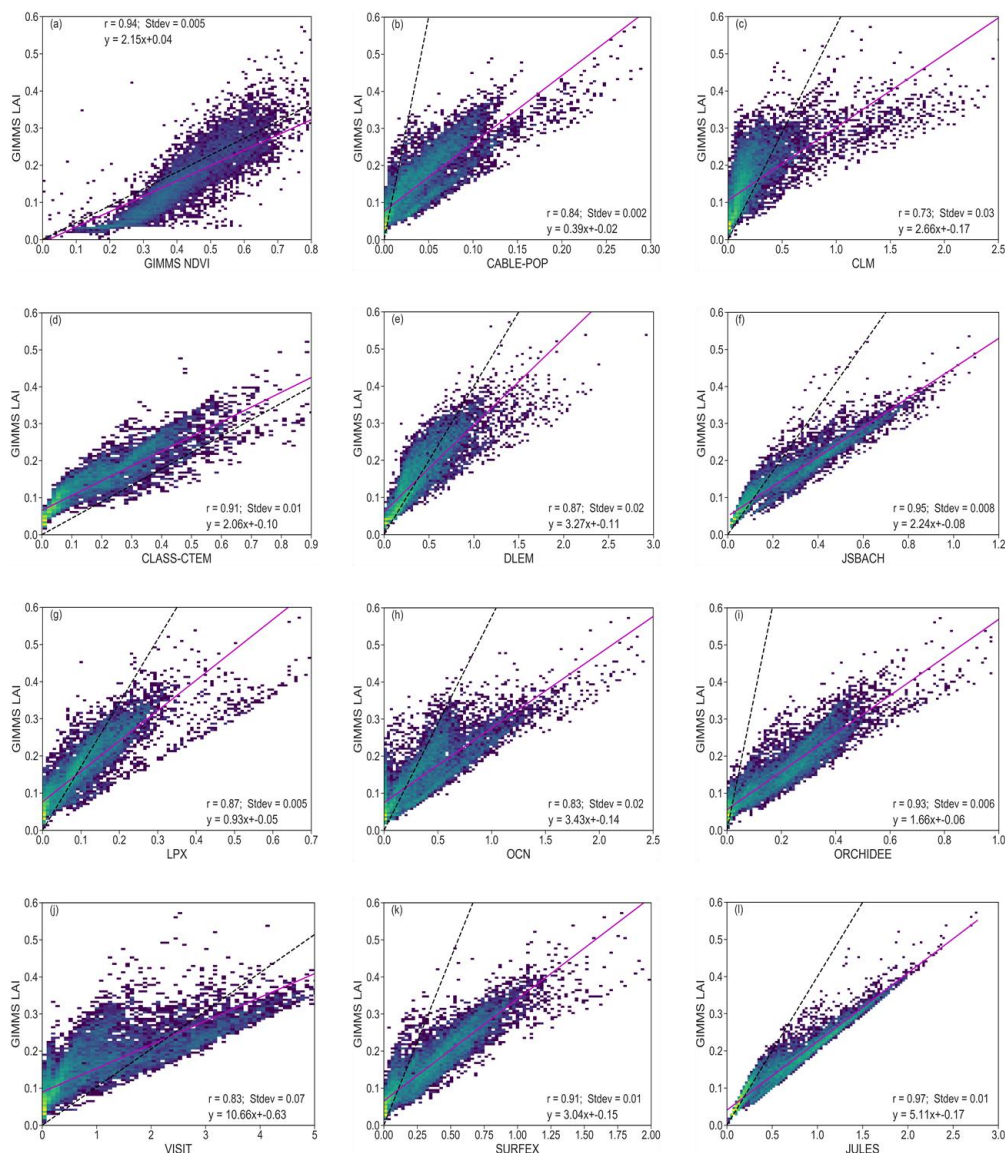
3.1 Grid cell correlations between NDVI and LAI

300 Figure 2 illustrates the relationships between NDVI and LAI for observations, as well as the
comparison between observed and model LAI. There is a strong linear relationship between
observed NDVI and LAI (Fig. 2a). It can be seen that the correlation (0.94) is high between both
variables and the standard deviation is low (0.005). From the figure, there is a log-like shape, where
NDVI grows faster when LAI is low (<0.2) and becomes saturated when LAI goes higher (>0.3).
305 A linear regression of the data shows a slope of 2.15. The low standard deviation indicates that the
values from the two indices are close and a standard lower deviation. Although there is a good
agreement between observed NDVI and LAI, the 1:1 line shows that the datasets are not exactly
equal to each other.

310 Furthermore, there is good agreement between observations and the simulated LAI (Fig. 2).
JULES and has the highest correlation (0.97) with observation (Fig. 2i). CLM has the weakest
(0.73) correlation with the observations (Fig. 2c). DLEM and LPX have the same correlation
coefficient value of 0.87 with observation (Fig. 2e, 2g). The positive relationships between
simulated and observed LAI indicate a general applicability in investigating the model's



315 performance of vegetation response to drought. It also shows that the correlation is strong enough
 to compare how the LAI reacts to drought in the ensemble. An aggregation of observation along
 the gradient of simulated LAI shows that most of the models have similar slopes with observation.



320

Figure 2. Scatterplots of correlations between vegetation indices (observation and model) for the period 1982 – 2011 over southern Africa. Inset values indicate the correlation coefficient (r) and standard deviation (Stdev). The color represents each grid cell. The pink solid line is the linear regression, while the dashed black line shows 1:1 line. The unequal x-axes is to visualize the detailed data for the models.

325

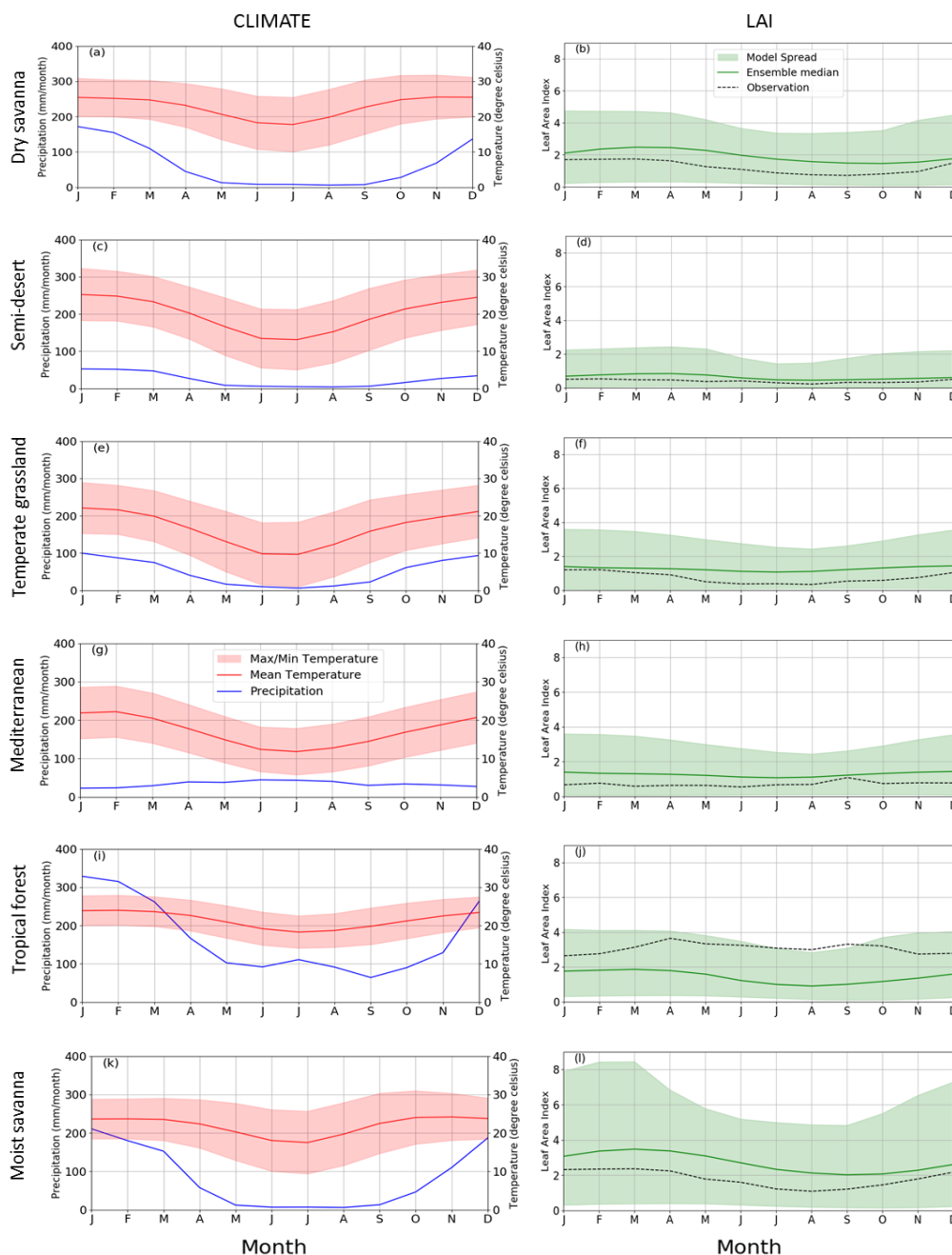


3.2 Climatology of observed and, simulated climate variables and LAI

This section compares the seasonal cycle of observation (CRU) and reanalysis (CRUJRA) climate variables; as well as observed and simulated LAI from GIMMS LAI and TRENDY models, respectively. Precipitation and temperature variables are seasonally variable and their climatologies are mostly similar. For example, precipitation is higher in MAM and DJF seasons over many of the biomes except in Mediterranean vegetation where precipitation is higher in JJA season. (Fig. 3a, 3b, 3e, 3i, 3k). The wettest month occurs over TF (i.e. tropical forest biome) where the precipitation is about 350mm. Conversely, during the dry season (JJA), there is little rainfall in the biome, although, it experiences some precipitation June and July months. Over the Mediterranean vegetation (Fig. 3g), a winter (JJA) rainfall region, rainfall variability is lower and is mostly dry in the DJF and SON. Similarly, the highest minimum and maximum temperature in the region is observed in the DJF season, where the highest temperature value exceeds 30°C. Over the tropical forest biome, although the distribution pattern of precipitation and temperature are similar for most months, they differ during June and July months. The pattern of precipitation and temperature distribution generally differ over the Mediterranean vegetation.

There are not strong patterns of seasonality in LAI, with maximum observed LAI values less than 4 in all biomes. The models well reproduce the climatology of LAI over the southern African biomes with a few exceptions (Fig. 3b, 3d 3f, 3h, 3j, 3l). For instance, the models simulate the drop in LAI over the semi desert, temperate grassland, tropical forest, dry savanna and moist savanna biomes in JJA season. The highest increase in observed LAI occurs over the tropical forest in April, although the models simulate a decrease in LAI over tropical forest during this time. On the other hand, lowest amount (less than 0.1) of LAI is observed in September and this occurs over the semi-desert biome. Observations typically fall within the range of the model ensemble. In addition, the distribution patterns of simulated LAI is similar to observation in most biomes except in the Mediterranean and tropical forest biomes. The LAI pattern also follows that of the climatic variables although the former lag behind.

355



360 Figure 3. Annual cycle of observed climate variables (precipitation, mm/month; maximum, minimum and mean temperature, °C) and LAI for observation and multi-model mean (TRENDY) across six southern African biomes over for the period 1982 – 2011. The annual cycle of the LAI for individual models are shown in Figure S5.



3.3 The evolution of drought in southern Africa

365

Figure 4 shows the evolution of observed SPEI in southern Africa between 1982 and 2011. Here, drought indices from CRUJRA are not included because preliminary investigation showed close magnitudes for drought indices computed from CRU and CRUJRA. We note that CRU was used to calculate SPEI for observation while simulated SPEI was computed with CRUJRA.

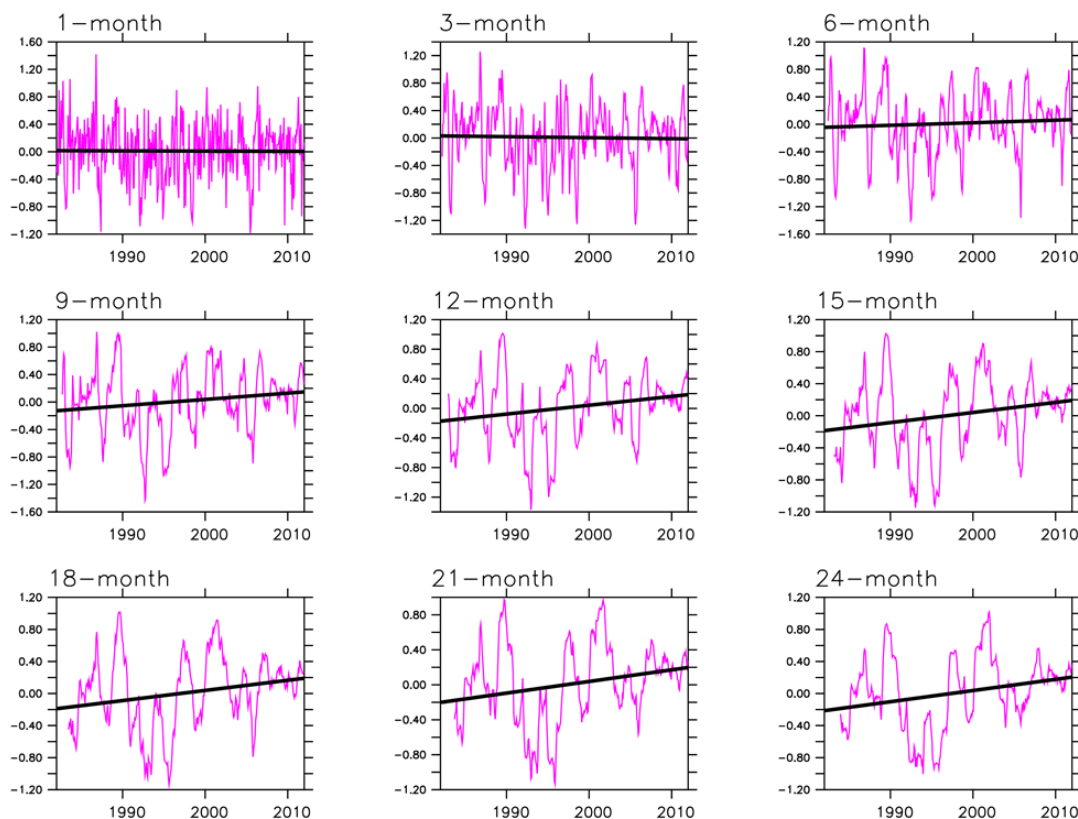
370

There is inter-annual, seasonal and decadal variability of the drought indices during dry and wet conditions over southern Africa. Although 1-, 3- and 6-month SPEI indicate no trend in wet or dry spells, they show the intensity of drought event for the 30-year period (Fig. 4a, 4b, 4c). The highest magnitude of drought is captured by 1-month SPEI while the lowest is shown in 21-month SPEI.

375

The severity of drought intensity is similar for all SPEI.

We note that the increasing trend in SPEI (9- to 24-month) does not imply that drought stress has decreased over time. There is need for more robust analysis to make such a conclusion.



380

Figure 4. Evolution of SPEI in southern Africa for the period 1982 – 2011. The trend is significant at 90% confidence interval for all timescales.



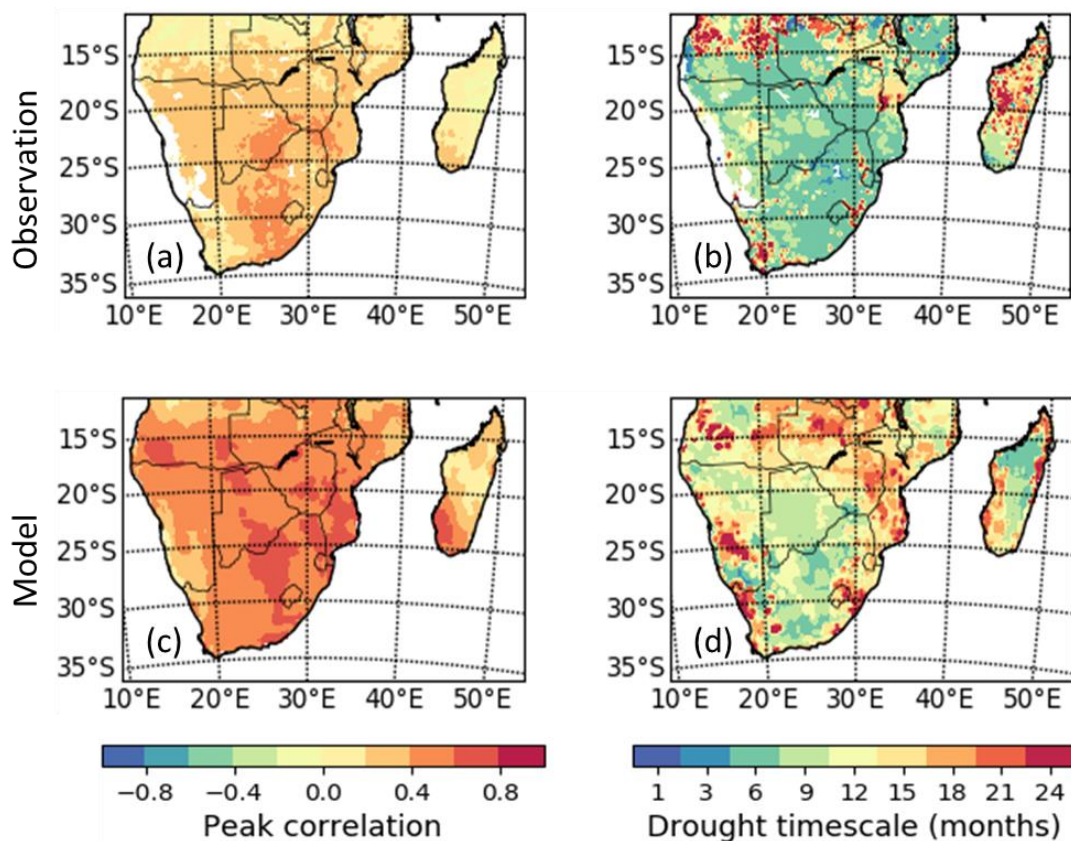
385 **3.4 Spatial distribution of LAI response to drought and the timescales**

Figure 5 presents the spatial distribution of the peak correlation between the SPEI and the LAI, and the timescales at which the correlation occurs. This is to show the magnitude of response of LAI to drought in southern Africa, and the length of the period for the response.

390 Observations show that southern African LAI can respond fairly strongly to droughts (peak
correlation magnitudes of between 0.4 and 0.6), though the response is much weaker (coefficient
of less 0.4) in eastern Madagascar, Angola and parts of South Africa (Fig. 5a). The TRENDY
multi model median generally overestimate the observed magnitude of the LAI to drought response
(Fig. 5c). Peak correlations for the models seem to be much stronger – in the 0.6-0.8 range for
395 most of the regions. In addition, over the arid areas of Namibia, models simulate a LAI while
observations depict no measurable LAI, indicating that models simulate the LAI in areas where
observations show no measurable LAI.

The multi model median have a drought timescale that is mostly longer than the observed (Fig. 5b,
d). For instance, drought response of simulated LAI occurs mostly over a longer time period (6-,
400 9-month timescale) than in the observation over eastern Madagascar. Over southern areas of
Madagascar and central Zambia, the multi model median overestimates the drought timescale.
Over central areas of South Africa and Mozambique, simulated LAI responds at intermediate (9-
month) timescales. However, similar drought timescales for the observation and the model
ensemble median are shown in parts of Angola.

405



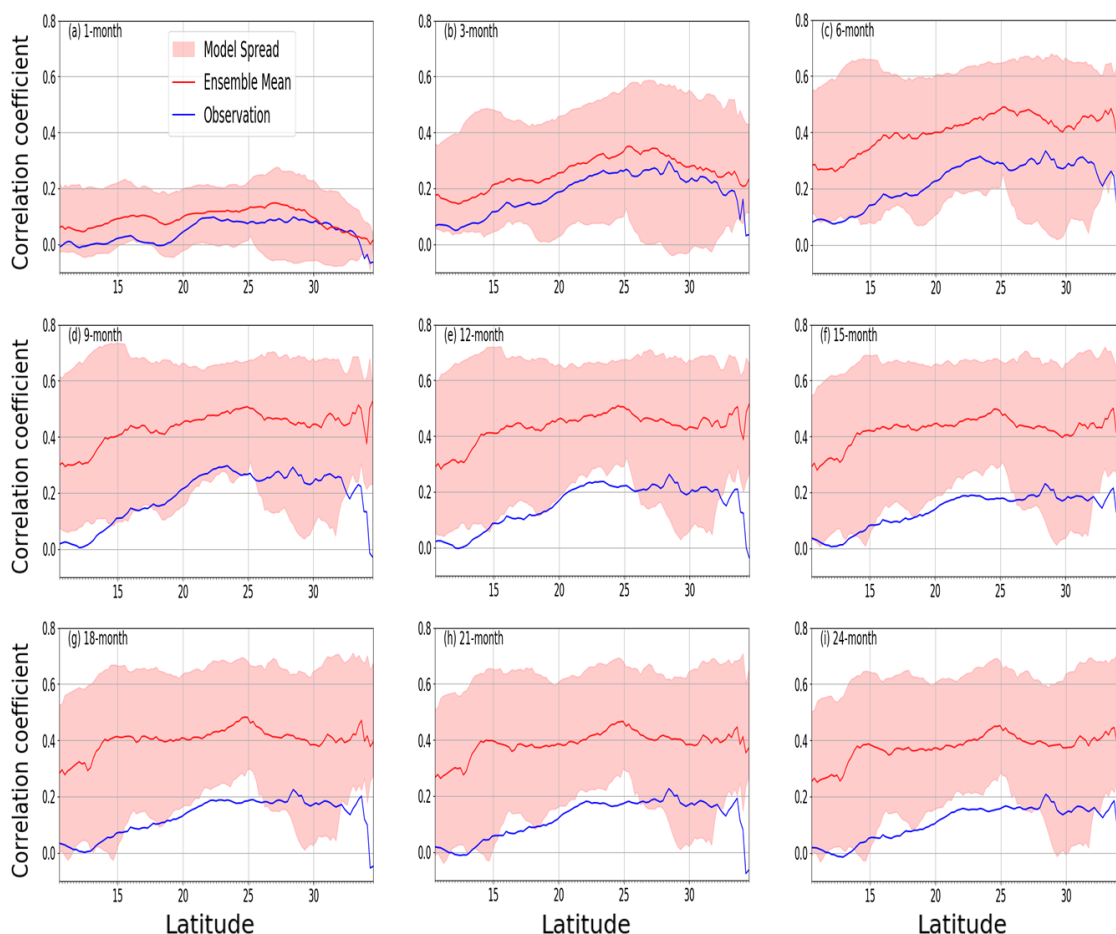
410 Figure 5. Spatial distribution of peak correlation between drought (SPEI) and LAI over the region
of southern Africa in the observation and in the model ensemble median; for the period 1982 –
2011. Panels (a) and (c) show the peak correlation per pixel, which is independent of the timescale
and the month of the year. Panels (b) and (d) indicate the timescales at which the peak correlation
between SPEI and LAI is found. Areas with no significant correlation are white.

415 3.5 Latitudinal distributions of LAI response to drought and the timescales

The present study investigated and discussed the implications of drought different
vegetation/biome types across latitudes in the region. While the pattern of the latitudinal
distribution of the LAI response to drought is identical across different timescales, the magnitudes
generally differ (Fig. 6). The response is much weaker (less than 0.15) for the 1-month timescale
than for other timescales. The strongest response is observed at 6-month timescales between
latitudes 25 and 30°. The model ensemble mean generally agrees with the pattern of the observed
LAI-SPEI correlations across all the timescales. However, the magnitudes differ from the
observation. Modeled correlation is stronger than observations for the longer (6-month or more)



425 timescales. Furthermore, there is an offset between observation and model mean which is consistent across most of the timescales, perhaps due to strong memory of the some of the models.



430 Figure 6. Mean correlation (observed and multi-model ensemble) of annual LAI and SPEI for 1982 – 2011 across latitudes over southern Africa for 1- to 24-month timescales.

3.6 Response of LAI to droughts across seasons

435 Observations show similar correlations between LAI and drought across all seasons in the biomes (Fig.7). For the dry savanna which is one of the most climate-impacted biomes in the region, LAI response to drought is strong and as high as 0.8 in MAM season and it occurs at 12-month timescale. The correlations between drought and LAI are also very strong in other seasons over the same biome and occur at 6- and 12-month drought timescale, except over the Mediterranean vegetation where the response occurs at 18-month in DJF season. Similarly, the peak correlations



440 between drought and LAI are strong across the other biomes. With exception of the tropical forest
biome, the drought timescale is at longer time periods (> 6-months).

The model ensemble generally overestimates the magnitude of correlations across the biomes in
the different seasons. Whilst the correlation magnitude remains mostly larger than the observed,
445 nonetheless, models simulate closer correlation with observation in some biomes and seasons. For
instance, over Mediterranean vegetation, models simulate fairly good response of LAI to drought
in all seasons. Furthermore, in nearly all other biomes, the ensemble spread overlaps with the
observations. In addition, simulations mostly overestimate drought timescale.

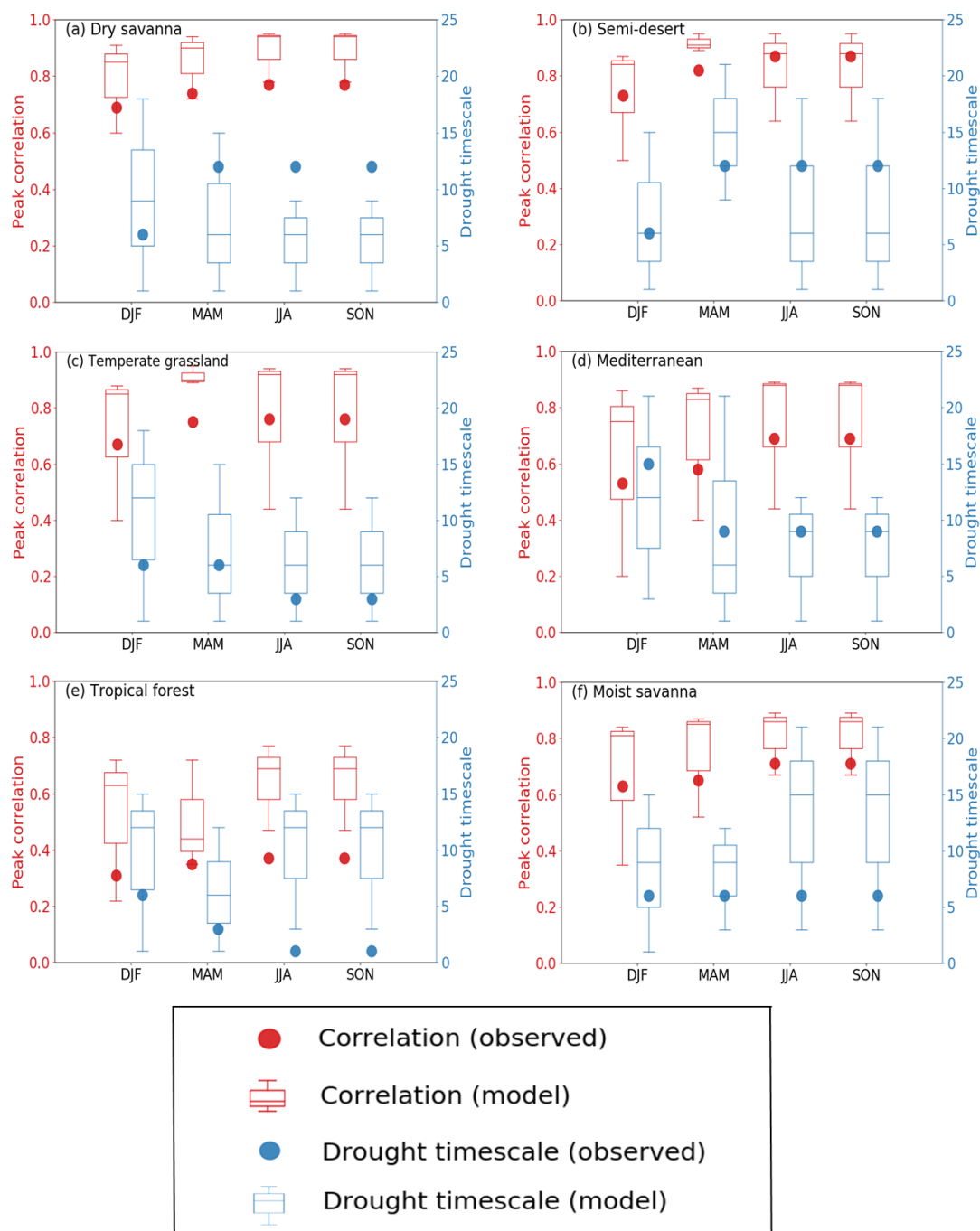
450

455

460

465

470



475 Figure 7. Seasonal correlations of drought (SPEI) and LAI across six southern African biomes. The values on the left axis show the peak correlation in observation and TRENDY models. The values on the right axis indicate the correlation drought timescale.



3.7 Inter-annual variation of model simulation of drought impacts on LAI

480 Table 1 shows correlations between observed mean SPEI and LAI for the period 1982 and 2011
 as well simulations by individual DGVM across different timescales. Unlike Fig. 5 which shows
 the peak correlations, the table shows the mean correlation for the 30-year period.

485 There is variation in the inter-annual simulation of LAI response to drought across different
 timescales by individual models. For instance, on the 1-month timescale, JULES simulates the
 least correlation value while JSBACH shows the highest correlation value. Furthermore, JSBACH
 simulates the highest correlation value for most of the timescales while CLM simulates the least
 correlation values for most (3-, 9-, 12-, 15- and 18-month) of the timescales.

Table 1. Model simulation of mean SPEI and LAI correlations between 1982 and 2011. * indicates
 the model with the lowest mean correlation.

Correl.	GIMMS LAI	CABLE- POP	CLM	CLASS- CTEM	DLEM	JSBACH	LPX	OCN	ORCHIDEE	SURFEX	JULES	VISIT
1-month	0.0066	0.1017	0.1188	0.1266	0.085	0.1388	0.0842	0.0579	0.0884	0.1094	0.027*	0.086
3-month	0.0775	0.3084	0.0187*	0.29	0.2499	0.4165	0.2403	0.1644	0.266	0.2791	0.1434	0.1108
6-month	0.091	0.3474	0.1806	0.3562	0.3305	0.5404	0.2386	0.3377	0.3733	0.3759	0.2429	0.1703*
9-month	0.0832	0.333	0.2034*	0.3496	0.3437	0.5734	0.2505	0.4055	0.39	0.3994	0.3189	0.23
12-month	0.0813	0.3053	0.2155*	0.3231	0.3229	0.5398	0.304	0.4109	0.4054	0.3911	0.3663	0.2892
15-month	0.0642	0.2773	0.2161*	0.2912	0.2846	0.4925	0.3208	0.4106	0.4132	0.3547	0.3623	0.3198
18-month	0.0452	0.2534	0.2349*	0.276	0.2381	0.4599	0.2405	0.3998	0.4109	0.3289	0.3586	0.3472
21-month	0.0406	0.239	0.2402	0.27	0.2119	0.4334	0.1569*	0.3739	0.3962	0.2955	0.3621	0.3501
24-month	0.0409	0.2302	0.2355	0.2668	0.2186	0.4696	0.2064*	0.3528	0.3777	0.2682	0.3617	0.327

490



3.8 Impacts of extreme events on LAI

The impact of extreme events on LAI is shown in Fig. 8. Here, extreme events are the wet years - i.e. the periods with precipitation higher than normal; and the dry years which include the periods of very high dry spells.

The magnitudes of response of LAI are generally stronger during the dry years than in wet years (Fig. 8). The distribution pattern of the magnitude of response however, varies across the region. With the exception of the year 2010, the strongest drought response is observed in parts of Namibia, Botswana, Tanzania and South Africa. During the 2010 wet year period, the response is weaker in most parts except northern part of Madagascar and southwestern part of South Africa (Figure 8F).

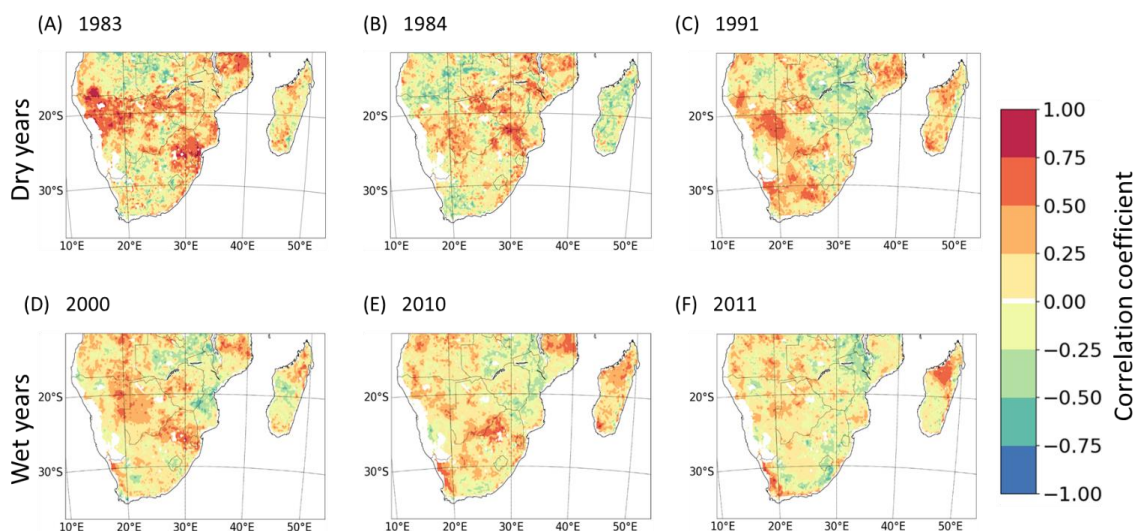


Figure 8. Spatial correlations of observed LAI response during extreme wet and dry years. For (A) – (C) changes were calculated as a difference between the wet year and the 30-year mean and for (D) – (F) between the dry year and the 30-year mean. White are areas with no correlation.

3.9 Comparison of global and regional distribution of LAI response to droughts (1982 – 2011)

There is variability in the global and regional temporal distribution of LAI response to drought (at 12-month timescale) when global vegetation biomes are split into regional biomes (Fig. 9). The map of the global biomes is shown in Fig. S1 in the supplementary material. The observed global response, indicates a decreasing trend of LAI while the model mean shows an increasing estimate.

The semi-desert biome dominates the LAI response as higher drought-vegetation correlations are observed (Figures 9G – I). Over the biome, there is more marked interannual variability which makes the biome an important player in global carbon cycling (Poulter *et al.*, 2014). The response

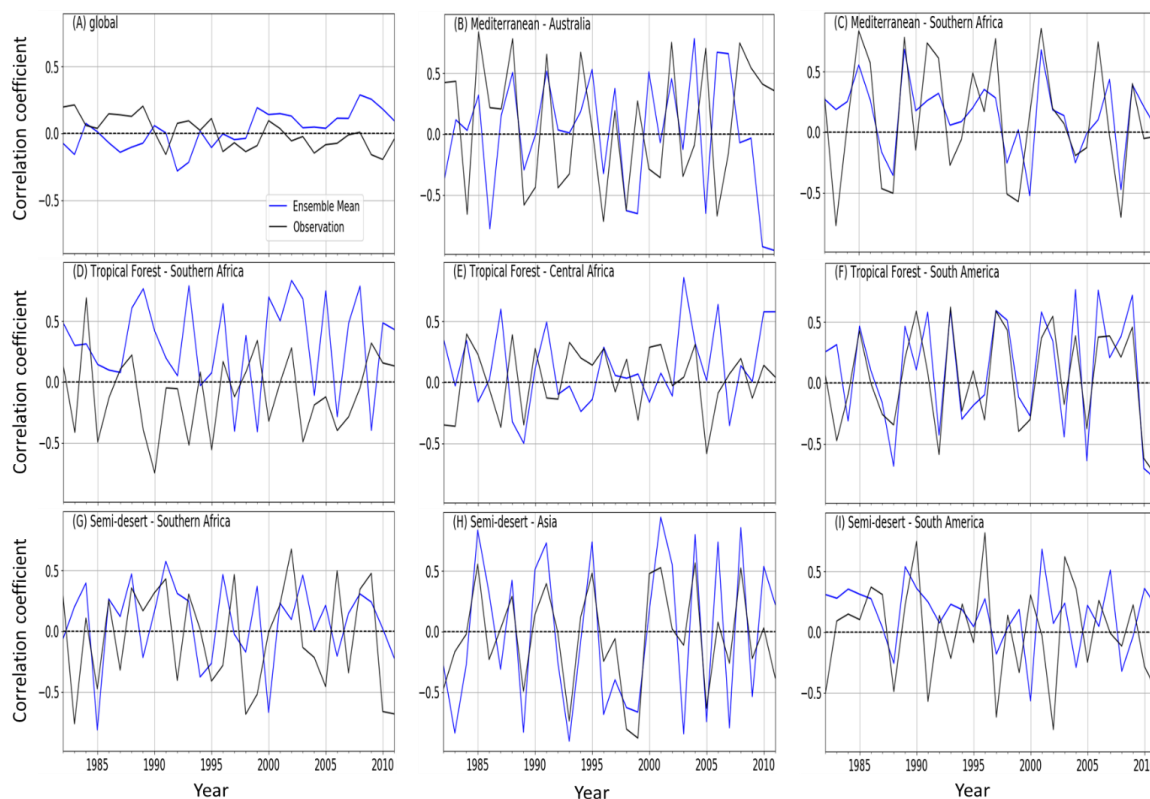


over the semi-desert in southern Africa is however weaker in comparison to the other semi-desert biomes.

520

The response over the Mediterranean vegetation in Australia is stronger than the Mediterranean vegetation over the rest of inland southern Africa. Over the biome, model simulates closer magnitudes in the latter than over Australia (Figures 9B and 9C).

525 Over the tropical forest biomes, there is a weaker response in Central Africa compared to Southern Africa and South America; the model simulates a closest response magnitude in South America (Figures 9D – F).



530 Figure 9. Correlations between SPEI (12-month timescale) and ensemble mean of LAI from
TRENDY (blue line), GIMMS LAI (black line) for (A) Global (B) Mediterranean vegetation over
Australia (C) Mediterranean vegetation over southern Africa (D) Tropical Forest over southern
Africa (E) Tropical Forest over Central Africa (F) Tropical Forest over South America (G) Semi-
535 desert biome over southern Africa (H) Semi-desert over Asia and (I) Semi-desert over South
America.



4 Discussion

4.1 Relationship of LAI to phenological changes

540 LAI is a variable that is needed for global modelling of biogeochemistry, climate, ecology and
hydrology and different primary production models (e.g., Running & Coughlan, 1988; Sellers *et*
al., 1996; Bonan, 1998). In view of the need to run biogeochemical models at regional and global
scales, accurate LAI data at moderate – high resolutions is crucial (Wang *et al.*, 2004). The
relationship between NDVI and LAI is applied as a support algorithm in MODIS LAI. Thus, from
545 the viewpoint of availability of data, retrieving LAI from analyzing NDVI-LAI relationship remain
the main perspective for high temporal resolution in regional and global-wide studies (Wang *et*
al., 2004).

LAI showed a linear relationship with NDVI. This suggests that the NDVI is associated with the
phenological changes of plants, the parts of surface cover class which contribute to the general
550 reflectance as well as the variations in the angle of solar zenith (Wang *et al.*, 2004). Studies (e.g.
Myoung *et al.*, 2013) have however, found that the relationship between NDVI and LAI varies
intra- and inter-annually. For instance, while the relationship is strong during periods of leaf
production and senescence, no relationship is observed during the period of leaf constant due to
NDVI saturation above certain LAI values (Xue and Su, 2017). Other studies have also shown that
555 the relationship between the two vegetation indices differs temporally and seasonally over
deciduous forests, which are sometimes not accounted for in models that test their relationship
(Wang *et al.*, 2004).

Our study analyzed the relationship between NDVI and LAI using spatiotemporal correlation
technique (See Fig. 2a). However, we note that using a single approach to evaluate the relationship
560 between both vegetation indices may be insufficient. This is due to the fact that deviations could
be introduced in the estimations of LAI and thus, estimations of carbon fluxes and balances (Wang
et al., 2004). Studies have suggested that various relationships should be used, for instance, in the
case of deciduous forest, the three stages of phenology such as leaf constant, leaf senescence and
leaf production, could be explored (Din *et al.*, 2017; Junges *et al.*, 2017). It has also been proposed
565 that, for the inter-annual variation, the relative NDVI should be used to evaluate inter-annual
variation in the relationship at different phenological stages (Hou *et al.*, 2015). Furthermore, other
studies have also recommended using correlation based on coefficients of regression and
environmental factors such as water availability, temperature, and soil factors (Glen *et al.*, 2008).
However, further study is required to test the viability of this approach. In addition, another method
570 that has been proposed is the coupling of various spectral vegetation indices from different
temporal scales into the regression analysis as this could add significant improvement over
regressions based only on one vegetation index (Cohen *et al.*, 2003).

Although the present study found a strong linear relationship between the NDVI and LAI in
southern Africa, other studies (Potitsep *et al.*, 2010; Pedro *et al.*, 2019) have shown the two indices
575 are not always directly proportional. For example, both indices do not exhibit the same
relationships over different eco-regions such as the Evergreen Broadleaf Forest, Deciduous
Needleleaf Forest. Furthermore, another study (Fan *et al.*, 2009; Tian *et al.*, 2016) found that the



LAI may be better indicator of plant biomass and health because of the saturation associated with the NDVI, particularly in drylands. This makes the LAI more applicable in monitoring vegetation response to drought. Evaluating how the LAI differs from the NDVI over different biomes (such as dry savanna, tropical forest, etc), with regards to temporal difference is shown in Fig. S6.

4.2 The importance of sub-monthly data in drought computation and monitoring

The data used to evaluate drought indices is CRUJRA. While CRUJRA is based on CRU, it is different because it is a reanalysis and has 6-hourly temporal resolution. Additionally, CRUJRA is the data used to force the DGVMs, so the drought indices are being calculated based on the same data the models use for their simulations. JRA is reanalysis but the combined product uses the sub-monthly information from JRA but is constrained to the monthly CRU observation. Please see Fig. S7 for the spatial comparisons of the data. It is useful to use data with shorter times because the study focuses on an evaluation of drought impact, which is sensitive to timescale. In drylands, for instance, the uncertainties associated with monthly data in drought monitoring are reduced when sub-monthly data are used (Mukherjee *et al.*, 2018).

4.3 Annual cycle of climate and vegetation in southern Africa

Climatologies of meteorological variables show that precipitation drops in JJA and SON seasons over the biomes except over Mediterranean vegetation. The dry condition that is experienced during these seasons could be attributed to the subtropical high pressure system which suppresses rainfall by shifting the ITCZ (the Inter-Tropical Convergence Zone) away from these regions (Naik and Abiodun, 2016).

Observations also show low LAI over some parts of southern Africa (please see Figure S2). The weak gradient in some parts of the region may be due to low winter rains produced by the frontal system which is not sufficient enough for growth of expanse vegetation (Lange *et al.*, 1999). The aridification of the western part of southern Africa may be attributed to the influence of cold sea surface temperature (SSTs) of the Namibian Upwelling system along the Namibian coasts (Ward *et al.*, 1983). The aridification does not only result in cessation of river discharge but also sediments that would have favored the growth of drier vegetation (Dupont, 2006).

4.4 LAI response to drought in observation

Drought is becoming frequent and more intense in southern Africa (Masih *et al.*, 2014). The frequent and stronger dry spells observed in Fig. 4 could be attributed to climate change. The severity and longer durations of drought have enormous impacts on the already endangered vegetation biomes in the region (Hoffman *et al.*, 2009). The results show that drought impacts on vegetation occur across the different seasons in the region. The seasonal difference in the response of vegetation to drought across biomes is influenced by numerous factors such as vegetation adaptive capacity and resilience, reproduction process, growth stage among others (Zeppel *et al.*, 2014; Corlett, 2016). For instance, over the tropical forest biome, drought has the least impact on vegetation in the region, which could be because of the deeper rooting system of the vegetation which allows them access to soil at the deeper water table (El-Vilaly *et al.*, 2017). It is reported



620 that major drivers of vegetation resilience and productivity are precipitation and temperature which
control the evapo-transpirative rate (Allen *et al.*, 2010). It is worth noting that vegetation in
southern Africa will be severely impacted if the trends continue in the same trajectory. For
instance, the regions where there is a strong vegetation response to drought are experiencing wood
encroachment and thus, will likely worsen based on the current trajectory of drought occurrence.

625 We note that the performance of drought indices is not only limited by the variables used in their
computation but also by biomes and location where they are used (Xu *et al.*, 2015). For example,
SPEI which is calculated using simple methods and has adaptable timescales performs better than
SPEI in arid regions (Bengueria *et al.*, 2014). However, SPEI which requires more variables for
its computation captures drought better in relatively humid zones (Bengueria *et al.*, 2014). SPEI is
630 however limited by the potential evapotranspiration (PET) because of its sensitivity to the variable
(Xu *et al.*, 2015).

The vegetation situated at the borders of Botswana-Namibia and Mozambique-Zambia respond to
droughts at an intermediate timescale (i.e. 9-month). The types of vegetation inhabiting these
regions, which are well adapted to water shortage because of their physiological and
morphological characteristics, takes prolonged period to respond to drought and thus, do not easily
635 shows symptoms of water strain (Vicente-Serrano *et al.*, 2013). The activities through which
vegetation minimize water loss include reduction in photosynthesis, reduced canopy cover
(Schwinning & Sala, 2004). The capacity for vegetation to store water is one adaptation for low
water ecosystems, as is reduced daytime stomatal conductance and CAM photosynthesis. The
disparity in the timescales spatial distribution in models from observation might be because the
640 parameters are represented and estimated in the models (Murray *et al.*, 2012). In addition, the
models are not similar in their drought timescales simulations.

The varying response of the tropical forests in different regions may be because of the interplay of
precipitation and temperature at different longitudes. Ahlstrom *et al.* (2015) showed that
temperature is particularly a strong factor in the response of this vegetation. Wang *et al.* (2018)
645 also reported that soil moisture variations play a key role in the magnitude of vegetation response.
The weak response of LAI to drought over Madagascar and Angola may be attributed to the fact
that the vegetation in these regions is able to store water for a long time which it uses during deficit
(Chapotin *et al.*, 2006). It may also be because rainfall is not the main regulatory component in the
growth of vegetation in these regions (Fuller and Prince, 1996). In regions such as Botswana and
650 Namibia, vegetation is highly dependent on water availability for their ecosystem functions
(Anyamba *et al.*, 2003). Please see Fig. S3 in the supplementary material for observed correlations
at different timescales.

The seasonal response of LAI to drought varies and this could be attributed to many factors. For
655 instance, the sensitivity of the semi-desert to water shortage makes them show quick response to
drought (New, 2015). The response is particularly stronger in the MAM season because it is during
this period that fruit, and develops leaves and biomass are produced by vegetation (Zeppel *et al.*,
2014). Critical water requirements by vegetation for these developmental activities in the MAM
season is the reason for the vegetation respond to droughts at a short timescale (Zeppel *et al.*,
660 2014). The strongest vegetation response (a correlation of about 0.92) is observed over the semi
desert biome (which is in the semi-arid environment) in the JJA season. This is a region with



665 vegetation which heavily depend on water for all their ecosystems functioning without which they would not survive (New, 2015). The drought response of tropical forest is weaker compared to all other biomes. Over the tropical forest biome, the fairly subtle drought response may be because the biome can be tolerant to drought, have stronger robust capacity and is therefore, not extremely impacted by droughts as are the other biomes (Gilgen *et al.*, 2005; Corlett, 2016).

670 The different response by the global biomes in different geographical locations may be because of climate variations and the sensitivity of LAI to climate variations (Ahlstrom *et al.*, 2015). The dominance of LAI response to drought over the semi-desert biome could be attributed to the global bush encroachment and is in consonance with the increasing greenness (Donohue *et al.*, 2009; Fensholt *et al.*, 2012; Andela *et al.*, 2013). Studies (Cai *et al.*, 2014; Trenberth *et al.*, 2014; Dai *et al.*, 2013; Wang *et al.*, 2014; Ahlstrom *et al.*, 2015) have also found that increased and frequent ENSO events due to climate change have not only led to the expansion of LAI but could increase 675 the water demand by semi-desert vegetation. This comparison is particularly important because until now, there has been little or no study on this.

4.5 How well drought and LAI response is represented in DGVM simulations

680 The observed LAI is simulated within the models and calculated by GIMMS based on Mao and Yan, 2019. Lu *et al.*, 2011 found that DGVMs perform better against observations than Earth system models (ESM) because they use observationally-derived climate and can include more complex representations of vegetation processes. The ESM is a coupled model simulating its own climate, while the individual DGVMs models used in the present study are standalone, i.e. are 685 applied with observational based meteorological forcing, and thus we remove one uncertainty. Since offline studies target the DGVM itself, removing one possible issue (incorrect climate drivers), it became imperative to use DGVM to study drought impacts.

690 DGVMs simulate the vegetation characteristics and impacts of climate on them. The validation of DGVM simulations of variables such as LAI is quite difficult. This is because of the unavailability of data on large spatiotemporal scale for the different vegetation classes (Potter and Klooster, 1998). Studies (e.g. Potter and Klooster, 1997) have also shown that errors present in the prediction of plant functional types (PFTs) tend to spread to biomass prediction in the model, thus possibly biasing estimates of carbon stored in terrestrial ecosystems. Nevertheless, the DGVMs used in this 695 study simulate the spatial patterns of vegetation distribution though with a magnitude bias as shown in Fig. S2 in the supplementary material.

700 TRENDY models mostly simulate the temporal patterns of global and regional distributions of LAI response to drought. The biases shown by the models have been attributed to the fact that the models do not factor land use changes (Ahlstrom *et al.*, 2015). This is evident in the simulation of LAI (please see Fig. S2).

705 The models' weaker simulation might also be because some of the DGVMs do not well reproduce the LAI magnitude. The negligible difference in the spatial distributions of SPEI of the models could be due to fact that the model PET does not play a strong role in drought occurrence in the southern Africa and that precipitation is the main driver of drought in the region. The variations in the characterization of hydrological processes in the models are also a source of uncertainty



because they reinforce the bifurcation in runoff outputs which has cascading effects on biospheric changes, evapotranspiration among others (Murray *et al.*, 2012; Stewart *et al.*, 2004). Also see Fig. S4 for correlations of the model ensemble median at different timescales. Another reason for the biases in the simulations may be to the design of the DGVM experimental set-up, which include the flux deviation between simulations without and with (Murray *et al.*, 2012).

5 Summary and conclusions

Southern African vegetation is continually affected by drought. In this study, we estimated the spatiotemporal characteristics of meteorological drought in southern Africa using the Standardized Precipitation Evapotranspiration Index (SPEI) over a 30-year period (1982 – 2011). The severity and drought impacts on vegetation production were examined at various drought time-scales (1- to 24-month timescales) by correlating drought index (SPEI) with GIMMS LAI at different timescales. We found that the LAI responds strongly ($r = 0.6$) to drought over the central and south eastern parts of the region, with weaker impacts ($r < 0.4$) over parts of Madagascar and Angola, mostly at a shorter time period (3-, 6-month timescale). For seasonal responses, semi-desert biome showed the strongest response ($r = 0.95$) to drought at 6-month timescale in the MAM season while the tropical forest biome shows the weakest response ($r = 0.35$) at 6-month timescale in the DJF season

We assessed the relationship between the NDVI and LAI by computing a grid cell correlation of NDVI and LAI, and also examined how well state of the art dynamic global vegetation models (DGVMs) simulate LAI and its response to drought. The DGVM multi-model ensemble mostly overestimated the spatial and seasonal distribution of LAI response to drought in most parts of the region. The results also show that:

- The relationship between the NDVI and LAI is linear thus implying that the vegetation index is connected to the changes in phenology of plant, reflectance and the angle of zenith variations from the surface cover class.
- The model ensemble shows biases in the correlation and timescale of LAI response to drought.
- The model ensemble overestimates observation on the seasonal distribution of vegetation – drought correlations across the different biomes.
- There is a stronger LAI response to drought in dry years than in wet years (for instance, in the year 1983 which was a dry year, $r > 0.84$ over Namibia and northeastern parts of South African but $r < 0.70$ in 2000, a wet year in same region); and a variability in the distribution patterns of global and regional response across biomes.

The present study has shown how the LAI responds to drought across the different southern African biomes. Given the present spatial coverage of space monitoring of vegetation in the region, the methods used in the study may be extended towards monitoring and characterizing the impacts



750 of droughts on land cover change, as this may permit real-time monitoring of extreme events on
terrestrial vegetation (Yin *et al.*, 2020; Moore *et al.*, 2018). The findings of this study (e.g.
timescales of LAI response to drought) could also be used for the development of drought early
warning systems in agriculture and forestry sectors. This will assist in the mitigation of direct and
indirect costs associated with vegetation production.

755 Furthermore, this study has applied eleven DGVMs to study how well DGVMs can reproduce the
response of LAI in southern African vegetation to drought. While this study may have provided
an insight into the capability of DGVMs to simulate vegetation response to drought. However, the
results of the study can however be improved in some ways. For example, we applied eleven
760 models from the TRENDY DGVMs. For future studies, the number of models should be increased,
perhaps from other model intercomparison experiments, because using more models might reduce
the level of uncertainty and biases in their simulation of drought response by vegetation. The
limitation of the DGVMs can be addressed optimizing the models so that their capability in
reproducing vegetation indexes is enhanced. In addition, there is a need to improve mechanistic
relationships in the models, which could be achieved by enhancing the model approximations
765 which had been done to achieve computational efficiencies (Transtrum, *et al.*, 2016). Furthermore,
simple phenomenological model could be developed from the complex model. These simple
models would use correlations among observations, unlike mechanistic relationships which exploit
causative individual constituent and suffer over-fitting problems (Transtrum, *et al.*, 2016). Lastly,
there may be need for hybridizing machine learning and mechanistic models (Fayyad *et al.*, 1996;
770 Mitchell, 1997) to simulate vegetation parameters. This is because machine learning models have
shown certain advantage in the prediction of outcomes of complex mechanisms by using databases
of inputs and outputs for a given task (Fayyad *et al.*, 1996; Mitchell, 1997).

775 *Data availability.* Sources of data used in this work are provided in Section 2.1 and comprise CRU,
CRUJRA, NDVI3g and Trendy DGVMs.

Author contributions. S.L. was responsible for conceptualization, developing the initial content of
the manuscript, including literature search, data analysis and writing of the manuscript. S.S. and
D.L. provided model outputs, and guided on data analysis. J.N., H.W.W., P.F, H.T. and B.H
780 provided guidance in terms of the article structure and finalization of the manuscript.

Competing interests. Authors declare no competing of interest.

785 *Acknowledgements.* The work was supported by the South African National Research Foundation
(NRF).

790



References

- 795 Allen, C.D., Macalady, A.K., Chenchouni, H., Bachelet, D., McDowell, N.; Vennetier, M., and
Gonzalez, P.: A global overview of drought and heat-induced tree mortality reveals
emerging climate change risks for forests, *For. Ecol. Manag.*, 259, 660–684,
<https://doi.org/10.1016/j.foreco.2009.09.001>, 2010.
- 800 Ahlström, A., Raupach, MR., Schurgers, G., Smith, B., Arneth, A., Jung, M., Reichstein, M.,
Canadell, JG., Friedlingstein, P., Jain, AK., Kato, E., Poulter, B., Sitch, S., Stocker, BD.,
Viovy, N., Wang, YP., Wiltshire, A., Zaehle, S., and Zeng, N.: The dominant role of semi-
arid ecosystems in the trend and variability of the land CO₂ sink, *Science*, 348, 895– 899,
<https://doi.org/10.1126/science.aaa1668>, 2015.
- 805 Andela, N., Liu, YY., van Dijk, A. I. J. M., de Jeu, R. A. M., and McVicar, T. R.: Global changes
in dryland vegetation dynamics (1988–2008) assessed by satellite remote sensing:
Comparing a new passive microwave vegetation density record with reflective greenness
data, *Biogeosciences* 10, 6657–6676, doi:10.5194/bg-10-6657-2013, 2013.
- Anyamba, A., Justice, CO., Tucker, CJ., and Mahoney, R.: Seasonal to interannual variability of
Vegetation and fires at SAFARI 2000 sites inferred from advanced very high resolution
Radiometer time series data, *Journal of Geophysical Research*, vol 10 no D13,
<https://doi.org/10.1029/2002JD002464>, 2003.
- 810 Beguería, S., Vicente-Serrano, SM., Reig, F., and Latorre, B.: Standardized precipitation
evapotranspiration index (SPEI) revisited: parameter fitting, evapotranspiration models,
tools, datasets and drought monitoring. *International Journal of Climatology* 34(10), 3001-
3023, <https://doi.org/10.1002/joc.3887>, 2014.
- 815 Bonan, G. B., Oleson, KW., Vertenstein, M., Lewis, S., Zeng, X., Dai, Y., Dickinson, DE., and
Yang, Z.: The land surface climatology of the NCAR land surface model coupled to the
NCAR community climate model, *Journal of Climate*, 11, 1307 – 1327,
<https://doi.org/10.1175/1520-0442.2002>.
- Chapotin, SM., Razanameharizaka, JH., and Holbrook, NM.: Water relations of baobab trees
(*Adansonia spp L.*) during the rainy season. Does stem water buffer daily water deficit.
820 *Plant and Cell Environment* 29, 1021-1032. doi. 10.1111-3040.2005.01456.x, 2006.
- Cai, W., Borlace, S., Lengaigne, M., van Rensch, P., Collins, M., Vecchi, G., Timmermann,
A., Santoso, A., McPhaden, MJ., Wu, M., England, L., H., Wang, G., Guilyardi, E., Jin, F.-
F: Increasing frequency of extreme El Nino events due to greenhouse warming. *Nat. Clim.*
Change 4, 111–116, doi:10.1038/nclimate2100, 2014.
- 825 Clark, D. B., Mercado, L. M., Sitch, S., Jones, C. D., Gedney, N., Best, M. J., Pryor, M., Rooney,
G. G., Essery, R. L. H., Blyth, E., Boucher, O., Harding, R. J., Huntingford, C., and Cox,
P. M.: The Joint UK Land Environment Simulator (JULES), model description – Part 2:
Carbon fluxes and vegetation dynamics, *Geosci. Model Dev.*, 4, 701–722,
<https://doi.org/10.5194/gmd-4-701-2011>, 2011.
- 830 Cohen, W. B., Maiersperger, T. K., Gower, S. T. and Turner, D. P.: An improved strategy
for regression of biophysical variables and Landsat ETM+ data., *Remote Sensing of*
Environment, 84: 561–571, [https://doi.org/10.1016/S0034-4257\(02\)00173-6](https://doi.org/10.1016/S0034-4257(02)00173-6), 2003
- Corlett, RT.: The Impacts of Droughts in Tropical Forests. *Trends Plant Sci* 21(7) 584-
593, <https://doi.org/10.1016/j.tplants.2016.02.003>, 2016.
- 835 Dai, A.: Drought under global warming: a review. *Wiley Interdisciplinary Reviews: Climate*
Change 2(1), 45–65, doi 10.1002/wcc.81, 2011.



- Dai, A.: Increasing drought under global warming in observations and models, *Nat. Clim. Change* **3**, 52–58, doi:10.1038/nclimate1633, 2013.
- 840 Din, M., Zheng, W., Rashid, M., Wang, S., and Shi, Z.: Evaluating Hyperspectral Vegetation Indices for Leaf Area Index Estimation of *Oryza sativa* L. at Diverse Phenological Stages, *Front. Plant Sci.*, **8**, doi/10.3389/fpls.2017.00820, 2017
- Donohue, R. J., McVicar, T. R., and Roderick, M. L.: Climate-related trends in Australian vegetation cover as inferred from satellite observations, 1981–2006. *Glob. Change Biol.* **15**, 1025–1039, doi:10.1111/j.1365-2486.2008.01746.x, 2009.
- 845 Dupont, LM.: Late Pliocene vegetation and Climate and Namibia (Southern Africa) derived From Palynology of ODP site 1082. *Geochemistry, Geophysics and Geosystems, An AGU Journal*. Vol 7 issue 5. doi: 10.1029/2005/gc001208, 2006.
- Earth Summit, United Nation Conference on Environment and Development.: <https://sustainabledevelopment.un.org/outcomedocuments/agenda21>, 1992.
- 850 El-Vilaly, M.A.S., Didan, K., Marsh, S.E., van Leeuwen, W.J., Crimmins, M.A., and Munoz, A.B.: Vegetation productivity responses to drought on tribal lands in the four corners region of the Southwest USA, *Front. Earth Sci.*, **12**, 37–51, doi. <https://doi.org/10.1007/s11707-017-0646-z>, 2017.
- 855 Fan, L., Gao, Y., Brück, H., and Bernhofer, Ch.: Investigating the relationship between NDVI and LAI in semi-arid grassland in Inner Mongolia using in-situ measurements *Theoretical and Applied Climatology*, 10.1007/s00704-007-0369-2, 2008.
- Fayyad, U., Piatetsky-Shapiro, G., Smyth, P. (Eds): *From data mining to knowledge discovery Databases*. *AI Magazine* **17**, 37. 1996.
- 860 Fensholt, R., Langanke, T., Rasmussen, K., Reenberg, A., Prince, S. D., Tucker, C., Scholes, R. J., Le, Q. B., Bondeau, A., Eastman, R., Epstein, H., Gaughan, A. E., Hellden, U., Mbow, C., Olsson, L., Paruelo, J., Schweitzer, C., Seaquist, J., and Wessels, K.: Greenness in semi-arid areas across the globe 1981–2007—an Earth Observing Satellite based analysis of trends and drivers, *Remote Sens. Environ.* **121**, 144–158. doi:10.1016/j.rse.2012.01.017, 2012.
- 865 FAO. 2000b (Eds). *FAO/ESAF Handbook for Defining and Setting up a Food Security Information and Early Warning System (FSIEWS)*. Rome
- Fuller, DO., and Prince, SD.: Rainfall and foliar dynamics in tropical southern Africa: Potential impacts of global climatic change on savanna vegetation, *Clim Change* **33**, 69–96. 10.1007/BF00140514, 1996.
- 870 Gielen, B., De Boeck, H., Lemmens, CMHM., Valcke, R., Nijs, I., and Ceulemans, R.: Grassland species will not necessarily benefit from future elevated air temperatures: a chlorophyll fluorescence approach to study autumn physiology. *Physiol Plant* **125**:52–63, doi:10.1111/j.1399-3054.2005.00539.x, 2005.
- 875 Gitelson, A. A.: Wide dynamic range vegetation index for remote quantification of biophysical characteristics of vegetation, *Journal of Plant Physiology*, vol. 161, no. 2, pp. 165–173, <https://doi.org/10.1078/0176-1617-01176>, 2004.
- Gitelson, A.A., Viña, A., Ciganda, V., Rundquist, D.C., and Arkebauer, T.J.: Remote estimation of canopy chlorophyll content in crops *Geophysical Research Letters*, **32**, p. L08403, 10.1029/2005GL022688, 2005.
- 880 Glantz, M.H., Betsill, M. and Crandall, K.: Food security in southern Africa. Assessing the



- use and value of ENSO information. National Center for Atmospheric Research, Boulder, CO, USA, 1997.
- 885 Goll, D. S., Vuichard, N., Maignan, F., Jornet-Puig, A., Sardans, J., Violette, A., Peng, S., Sun, Y., Kvakic, M., Guimberteau, M., Guenet, B., Zaehle, S., Penuelas, J., Janssens, I., and Ciais, P.: A representation of the phosphorus cycle for ORCHIDEE, *Geosci. Model Dev.*, 10, 3745–3770, <https://doi.org/10.5194/gmd-10-3745-2017>, 2017.
- Hao, Z., and AghaKouchak, A.: Multivariate standardized drought index: a parametric multi-index model, *Advances in Water Resources*, 57, 12– 18., <https://doi.org/10.1016/j.advwatres.2013.03.009> 2013
- 890 Haverd, V., Smith, B., Nieradzik, L., Briggs, P. R., Woodgate, W., Trudinger, C. M., Canadell, J. G., and Cuntz, M.: A new version of the CABLE land surface model (Subversion revision r4601) incorporating land use and land cover change, woody vegetation demography, and a novel optimisation-based approach to plant coordination of photosynthesis, *Geosci. Model Dev.*, 11, 2995– 3026, [https://doi.org/10.5194/gmd-11-](https://doi.org/10.5194/gmd-11-2995-2018)
- 895 2995-2018, 2018.
- Harris, I., Jones, PD., Osborn, TJ., and Lister, DH.: Updated high-resolution grids of monthly climatic observations – the CRU TS3.10 Dataset. *Int. J. Climatol.* 34(3), 623–642, doi: 10.1002/joc.3711, 2014.
- Hoffman, MT., Carrick, PJ., and West, AG.: Drought, climate change and vegetation response in the succulent karoo, South Africa. *South African Journal of Science S.Afr. j. sci.* vol05:1-2, S. Afr. j. sci. vol.105 n.1-2 Pretoria Jan./Feb., 2009
- 900 Homdee, T., Pongput, K., and Kanae, S.: A comparative performance analysis of three standardized climatic drought indices in the Chi River basin, Thailand. *Agriculture and Natural Resources*, 50(3), 211– 219. <https://doi.org/10.1016/j.anres.2016.02.002>, 2016.
- 905 Hou, W., Gao, J., Wu, S., Dai, E.: Interannual Variations in Growing-Season NDVI and Its Correlation with Climate Variables in the Southwestern Karst Region of China. *Remote Sens.*, 7, 11105-11124, <https://doi.org/10.3390/rs70911105>, 2015.
- Ji, L., and Peters, AJ.: Performance evaluation of spectral vegetation indices using a statistical sensitivity function. *Remote Sensing of Environment* 106, 59–65, <https://doi.org/10.1016/j.rse.2006.07.010> 2007.
- 910 Junges, A. H., Fontana, D., Anzanello, R. and Bremm, C.: Normalized difference vegetation index obtained by ground-based remote sensing to characterize vine cycle in Rio Grande do Sul, Brazil. *Ciência e Agrotecnologia*, 41, 543-553. <https://doi.org/10.1590/1413-70542017415049016>, 2017.
- 915 Khosravi, H., Haydari, E., Shekoohizadegan, S., and Zareie, S.: Assessment the effect of drought on vegetation in desert area using landsat data Egypt. *J. Remote Sens. Space Sci.*, 2007 (20), pp. S3-S12 ISSN 1110-9823, <https://doi.org/10.1016/j.ejrs.2016.11.007>, 2017.
- Kato, E., Kinoshita, T., Ito, A., Kawamiya, M., and Yamagata, Y.: Evaluation of spatially explicit emission scenario of landuse change and biomass burning using a process-based biogeochemical model, *Journal of Land Use Science*, 8, 104–122, <https://doi.org/10.1080/1747423X.2011.628705>, 2013.
- 920 Kwon, M., Kwon, H.H., Han, D.: Spatio-temporal drought patterns of multiple drought indices based on precipitation and soil moisture: a case study in South Korea *Int. J. Climatol.*, 1–19 (2019), 10.1002/joc.6094, 2019.
- 925 Lake PS (eds) (2011). *Drought and Aquatic Ecosystems: Effects and Response*



- 930 Lange, C. B., Berger, W. H., Lin, H.-L., Wefer, G. and Shipboard Scientific Party Leg
175.: The early Matuyama diatom maximum off SW Africa, Benguela current system
(ODP Leg 175), *Mar. Geol.*, 161, 93–114, [https://doi.org/10.1016/S0025-3227\(99\)00081-X](https://doi.org/10.1016/S0025-3227(99)00081-X), 1999
- Lawal S., Lennard C., Jack C. Wolski P., Hewitsin B., and Abiodun B.: The observed and
model-simulated response of southern African vegetation to drought.
<https://doi.org/10.1016/j.agrformet.2019.107698>, 2019.
- 935 Lawal S., Lennard C and Hewitson B.: Response of southern African vegetation to climate
change at 1.5 and 2.0 degrees global warming above the pre-industrial level. *Climate
Services* 16C 100134, 2019.
- Le Quéré, C., Peters, G. P., Andres, R. J., Andrew, R. M., Boden, T. A., Ciais, P.,
Friedlingstein, P., Houghton, R. A., Marland, G., Moriarty, R., Sitch, S., Tans, P., Arneeth,
A., Arvanitis, A., Bakker, D. C. E., Bopp, L., Canadell, J. G., Chini, L. P., Doney, S. C.,
940 Harper, A., Harris, I., House, J. I., Jain, A. K., Jones, S. D., Kato, E., Keeling, R. F., Klein
Goldewijk, K., Körtzinger, A., Koven, C., Lefèvre, N., Maignan, F., Omar, A., Ono, T.,
Park, G.-H., Pfeil, B., Poulter, B., Raupach, M. R., Regnier, P., Rödenbeck, C., Saito, S.,
Schwinger, J., Segschneider, J., Stocker, B. D., Takahashi, T., Tilbrook, B., van Heuven,
S., Viovy, N., Wanninkhof, R., Wiltshire, A., and Zaehle, S.: Global carbon budget 2013,
945 *Earth Syst. Sci. Data*, 6, 235–263, <https://doi.org/10.5194/essd-6-235-2014>, 2014.
- Lienert, S., and Joos, F.: A Bayesian ensemble data assimilation to constrain model parameters
and land-use carbon emissions, *Biogeosciences*, 15, 2909–2930,
<https://doi.org/10.5194/bg-15-2909-2018>, 2018.
- 950 Lu, E., Luo, Y., Zhang, R., Wu, Q., and Liu, L.: Regional atmospheric anomalies responsible
for the 2009–2010 severe drought in China, *J. Geophys. Res.*, 116 (D21),
<https://doi.org/10.1029/2011JD015706>, 2011.
- Lu, E., Cai, W., Jiang, Z., Zhang, Q., Zhang, C., Higgins, R.W., and Halpert, M.S.: The day-to-
day monitoring of the 2011 severe drought in China, *Clim. Dynam.*,
<https://doi.org/10.1007/s00382-013-1987-2>, 2014.
- 955 Mao, J., and Yan, B.: Global Monthly Mean Leaf Area Index Climatology, 1981-2015.
ORNL DAAC, Oak Ridge, Tennessee, USA. <https://doi.org/10.3334/ORNLDAAC/1653>,
2019.
- Masih, I., Uhlenbrook, S., Maskey, S., and Smakhtin, V.: Stream-flow trends and climate
960 linkages in the Zagros Mountain, Iran. *Clim. Change*, 104, 317–338, doi:10.1007/s10584-
009-9793-x, 2011, 2014.
- Mauritsen, T., Bader, J., Becker, T., Behrens, J., Bittner, M., Brokopf, R., Brovkin, V.,
Claussen, M., Crueger, T., Esch, M., Fast, I., Fiedler, S., Popke, D., Gayler, V., Giorgetta,
M., Goll, D., Haak, H., Hagemann, S., Hedemann, C., Hohenegger, C., Ilyina, T., Jahns,
T., Jimenez Cuesta de la Otero, D., Jungclaus, J., Kleinen, T., Kloster, S., Kracher, D.,
965 Kinne, S., Kleberg, D., Lasslop, G., Kornblüeh, L., Marotzke, J., Matei, D., Meraner, K.,
Mikolajewicz, U., Modali, K., Möbis, B., Müller, W., Nabel, J. E. M. S., Nam, C., Notz,
D., Nyawira, S., Paulsen, H., Peters, K., Pincus, R., Pohlmann, H., Pongratz, J., Popp, M.,
Raddatz, T., Rast, S., Redler, R., Reick, C., Rohrschneider, T., Schemann, V., Schmidt,
H., Schnur, R., Schulzweida, U., Six, K., Stein, L., Stemmler, I., Stevens, B., von Storch,
970 J., Tian, F., Voigt, A., de Vrese, P., Wieners, K.-H., Wilkenskjaeld, S., Roeckner, E., and
Winkler, A. Developments in the MPI-M Earth System Model version 1.2 (MPI-ESM1.2)



- and its response to increasing CO₂, *J. Adv. Model. Earth Sy.*,
<https://doi.org/10.1029/2018MS001400>, 2018.
- 975 McKee, T. B., Doesken, N. J. and Kleist, J.: The relationship of drought frequency and
duration to time scales. *Proc. Eight Conf. on Applied Climatology*. Anaheim, CA, Amer.
Meteor. Soc. 179–184, 1993
- Melillo, J.: Climate change, risky business, and a call to action for ecologists. *Ecosystem
Health and Sustainability* 1(1), <https://doi.org/10.1890/EHS14-0016.1>, 2015.
- 980 Melton, J. R., and Arora, V. K.: Competition between plant functional types in the Canadian
Terrestrial Ecosystem Model (CTEM) v. 2.0, *Geosci. Model Dev.*, 9, 323–361,
<https://doi.org/10.5194/gmd-9-323-2016>, 2016.
- Mitchell TM. 1997 *Machine learning*. Boston, MA: McGraw-Hill Series in Computer Science.
- Mitchell, TD., and Jones, PD.: An improved method of constructing a database of monthly
climate observations and associated high- resolution grids. *Int. J. Climatol.* 25: 693–712,
985 <https://doi.org/10.1002/joc.1181>, 2005.
- Moore, B., Crowell, S. M. R., Rayner, P. J., Kumer, J., O'Dell, C. W., O'Brien, D., Utembe,
S., Polonsky, I., Schimel, D., and Lemen, J.: The potential of the geostationary carbon
cycle observatory (GeoCarb) to provide multi-scale constraints on the carbon cycle in the
Americas. *Frontiers in Environmental Science*, 6, 109,
990 <https://doi.org/10.3389/fenvs.2018.00109>, 2018.
- Mukherjee, N., Zabala, A., Huge, J., Nyumba, T. O., Esmail, B. A., and Sutherland, W.
J.: Comparison of techniques for eliciting views and judgements in decision-
making. *Methods in Ecology and Evolution*, 9, 54– 63, <https://doi.org/10.1111/2041-210X.12940>, 2017.
- 995 Murray, SJ., Foster, PN., and Prentice, IC.: Evaluation of global continental hydrology as
simulated by the Land-surface Processes and eXchanges Dynamic Global Vegetation
Model. *Hydrology and Earth System Sciences* 15: 91–105, <https://doi.org/10.5194/hess-15-91-2011>, 2011.
- Myoung, B., Choi, Y.-S., Hong, S., and Park S. K.: Inter- and intra-annual variability of
1000 vegetation in the northern hemisphere and its association with precursory meteorological
factors, *Global Biogeochem. Cycles*, 27, 31– 42, doi:10.1002/gbc.20017, 2013.
- Naik, M., and Abiodun, BJ.: Potential impacts of forestation on future climate change in
Southern Africa. *International Journal of Climatology*. doi:10.1002/joc.4652, 2016.
- Naumann, G., Alfieri, L., Wyser, K., Mentaschi, L., Betts, R.A., Carrao, H., Spinoni, J., Vogt, J.,
1005 Feyen, L.: Global changes in drought conditions under different levels of
warming. *Geophys. Res. Lett.*, 45, 3285–3296., <https://doi.org/10.1002/2017GL076521>,
2018.
- New, M.: Are semi-arid regions climate change hot-spots? Evidence from Southern Africa,
African Climate and Development Initiative (ACDI) blog, 2015.
- 1010 Oleson, K. W., Dai, Y., Bonan, G., Bosilovich, M., Dickinson, R., Dirmeyer, P., Hoffman, F.,
Houser, P., Levis, S., Niu, G.-Y., Thornton, P., Vertenstein, M., Yang, Z.-L. and Zeng,
X.: Technical description of the Community Land Model (CLM). NCAR Tech. Note
NCAR/TN-461+STR, 174 pp, 2004.
- 1015 Oleson, K., Lawrence, D., Bonan, G., Drewniak, B., Huang, M., Koven, C., Levis, S., Li, F.,
Riley, W., Subin, Z., Swenson, S., Thornton, P., Bozbiyik, A., Fisher, R., Heald, C.,
Kluzek, E., Lamarque, J., Lawrence, P., Leung, L., Lipscomb, W., Muszala, S., Ricciuto,
D., Sacks, W., Tang, J., and Yang, Z.: Technical Description of version 4.5 of the



- Community Land Model (CLM), NCAR, available at:
http://www.cesm.ucar.edu/models/cesm1.2/clm/CLM45_Tech_Note.pdf, 2013.
- 1020 Palmer WC.: Keeping track of crop moisture conditions, nationwide: the new Crop Moisture Index. *Weatherwise* 21:156–161, <https://doi.org/10.1080/00431672.1968.9932814>, 1968.
- Pinzon, J. E. and Tucker, C. J.: A Non-Stationary 1981-2012 AVHRR NDVI3g Time Series, *Remote Sensing*, 6, 6929–6960, <https://doi.org/10.3390/rs6086929>, 2014.
- 1025 Potitthep, S., Nasahara, N., Muraoka, H., Nagai, S. and Suzuki, R.: What is the actual relationship between LAI and VI in a deciduous broadleaf forest. *International Archives of the Photogrammetry, Remote Sensing and Spatial Information Science* 38, 609–614, 2010.
- Poulter, B., Frank, D., Ciais, P., Myneni, R. B., Andela, N., Broquet, G. J. B., Canadell, J. G., Chevallier, F., Liu, Y. Y., Running, S. W., Sitch, S., and van der Werf, G. R.: Contribution of semi-arid ecosystems to interannual variability of the global carbon cycle. *Nature* 509, 600–603, doi:10.1038/nature13376pmid:2484788, 2014.
- 1030 Potter, C.S., and Klooster, S.A.: Global model estimates of carbon and nitrogen storage in litter and soil pools: response to change in vegetation quality and biomass allocation. *Tellus*, 49B, 1, <https://doi.org/10.3402/tellusb.v49i1.15947>, 1997.
- 1035 Potter, CS, and Klooster, SA.: Dynamic global vegetation modelling for prediction of plant types and biogenic trace gas fluxes. *Global Ecol Biogeogr* 8:473–488, <https://doi.org/10.1046/j.1365-2699.1999.00152.x>, 1998
- Running, S. W., & Coughlan, J. C.: A general model of forest ecosystem processes for regional applications. *Ecological Modelling*, 42, 124 – 154., [https://doi.org/10.1016/0304-3800\(88\)90112-3](https://doi.org/10.1016/0304-3800(88)90112-3), 1988.
- 1040 Santin-Janin, H., Garel, M., Chapuis, J.-L., and Pontier, D.: Assessing the performance of NDVI as a proxy for plant biomass using non-linear models: a case study on the Kerguelen archipelago *Polar Biology*, 32 (2009), pp. 861-871, <https://doi.org/10.1007/s00300-009-0586-5>, 2009.
- 1045 Schwinning, S., Starr, B. I., and Ehleringer, J. R., Summer and winter drought in a cold desert ecosystem (Colorado Plateau) part II: effects on plant carbon assimilation and growth. *Journal of Arid Environments* 61:61–78., <https://doi.org/10.1016/j.jaridenv.2004.07.013>, 2005.
- Sinclair, REA., and Beyers, RL.: African Biomes. *Ecology*. doi.10.10/OBO978199830060., 2015.
- 1050 Sellers, P. J., Randall, D. A., Collatz, G. J., Berry, J. A., Field, C. B., Dazlich, D. A., Zhang, C., and Collelo, GD., and Bounoua, L.: A revised land surface parameterization (SIB2) for Atmospheric GCMs: Part I. Model formulation. *Journal of Climate*, 9, 676 – 705., <https://doi.org/10.1175/1520-0442.1996>.
- 1055 Scott, R.: Using watershed water balance to evaluate the accuracy of eddy covariance evaporation measurements for three semiarid ecosystems, *Agr. For. Meteorol.*, 150, 219–225, doi:10.1016/j.agrformet.2009.11.002., 2010.
- Sitch, S., Huntingford, C., Gedney, N., Levy, P.E., Lomas, M., Piao, S.L., Betts, R., Ciais, P., Cox, P., Friedlingstein, P., Jones, CD., Prentice, IC., and Woodward, FI.: Evaluation of the terrestrial carbon cycle, future plant geography and climate-carbon cycle feedbacks using five Dynamic Global Vegetation Models (DGVMs). *Global Change Biol.*, 14, 2015– 2039, <https://doi.org/10.1111/j.1365-2486.2008.01626.x>, 2008.
- 1060 Stage, J. H., Tallaksen, L.M., Gudmundsson, L., van Loon, A.F. and Stahl, K.: Pan-European comparison of candidate distributions for climatological drought indices (SPI



- 1065 and SPEI) Hydrology in a Changing World: Environmental and Human Dimensions
Proceedings of FRIEND -Water 2014, Montpellier, France, October 2014 (IAHS Publ.
363, 2014.
- Stewart, IT., Cayan, DR., Dettinger, MD.: Changes in snowmelt runoff timing in western
North America under a ‘business as usual’ climate change scenario. *Climatic Change* 62(1–
3): 217–232., <https://doi.org/10.1023/B:CLIM.0000013702.22656.e8>, 2004.
- 1070 Sultan, B., and Gaetani, M.: Agriculture in West Africa in the twenty-first century: Climate
change and impacts scenarios, and potential for adaptation. *Frontiers in Plant
Science*, 7, 1– 20, doi: 10.3389/fpls.2016.01262, 2016
- Tian, F., Brandt, M., Liu, Y. Y., Rasmussen, K., and Fensholt, R.: Mapping gains and losses
in woody vegetation across global tropical drylands. *Global Change*
1075 *Biology*, 23(4), 1748– 1760. <https://doi.org/10.1111/gcb.13464>, 2017.
- Transtrum, MK., Qiu, P.: Bridging mechanistic and phenomenological models of complex
biological systems. *PLoS Comput Biol* 12(5):e1004, 915,
<https://doi.org/10.1371/journal.pcbi.1004915>, 2016.
- 1080 Trenberth, K. E., A. Dai, G. van der Schrier, P. D. Jones, J. Barichivich, K. R. Briffa, and J.
Sheffield.: Global warming and changes in drought, *Nat. Clim.
Change*, 4(1), 17– 22., <https://doi.org/10.1038/nclimate2067>, 2014.
- Teuling, AJ., vanLoon A., Seneviratne S., Lehner, M., Aubinet M., Heinesch B., Bernhofer,
C., Grunwald, T., Prasse, H., and Spank, U.: Spank Evapotranspiration amplifies
European summer drought *Geophys. Res. Lett.*, 40 (10), pp. 2071-2075,
1085 <https://doi.org/10.1002/grl.50495>, 2013.
- Tian, H. Q., Chen, G. S., Lu, C. Q., Xu, X. F., Hayes, D. J., Ren, W., Pan, S. F., Huntzinger,
D. N., and Wofsy, S. C.: North American terrestrial CO₂ uptake largely offset by CH₄
and N₂O emissions: toward a full accounting of the greenhouse gas budget, *Climatic
Change*, 129, 413–426, <https://doi.org/10.1007/s10584-014-1072-9>, 2015.
- 1090 Ujeneza, E., and Abiodun, BJ., Drought regimes in Southern Africa and how well GCMs
simulate them? *Clim Dyn*, 44 (5), 1595-1609, [10.1007/s00382-014-2325-z](https://doi.org/10.1007/s00382-014-2325-z), 2015.
- United Nations Environmental Protection – UNEP (2008). Atlas of changing environment.
Biomes of Africa. *Nairobi, Kenya: UNEP*.
- 1095 Vicente-Serrano, SM., Beguería, S., López-Moreno, JI., Angulo, M. El Kenawy, A.: A new
global 0.5° gridded dataset (1901-2006) of a multiscalar drought index: comparison with
current drought index datasets based on the Palmer Drought Severity Index. *Journal of
Hydrometeorology* 11: 1033–1043, <https://doi.org/10.1175/2010JHM1224.1>, 2010.
- Vicente-Serrano, S. M, Bengueria, S., and Lopez-Moreno, J.: Comment on ‘‘Characteristics and
trends in various forms of the Palmer Drought Severity Index (PDSI) during 1900–2008’’
1100 by Aiguo Dai. *J. Geophys. Res.*, 116, D19112, doi:10.1029/2011JD016410, 2011.
- Vicente-Serrano, SM., Gouvelia, C., Camarero, J.J, Begueria, S., Trigo, R., Lopez-Moreno, JI.,
Azorin-Molina, A., Pasho, E., Lorenzo-Lacruz., J, Revuelto, J., Moran-Tejeda, E., and
Sanchez-Lorezo, A.: Response of vegetation to drought time-scales across global land
biomes. *PNAS Vol 110 1*. www.pnas.org/cgi/doi/10.1073/pnas.1207068110, 2012.
- 1105 Vicente-Serrano, Sergio M. and National Center for Atmospheric Research Staff (Eds):
"The Climate Data Guide: Standardized Precipitation Evapotranspiration Index (SPEI)."
Retrieved from [https://climatedataguide.ucar.edu/climate-data/standardized-precipitation-
evapotranspiration-index-spei](https://climatedataguide.ucar.edu/climate-data/standardized-precipitation-evapotranspiration-index-spei)., 2015.
- Wang, Q., Tenhunen, J., Dinh, NQ., Reichstein, M., Vesala, T., and Keronen, P.: Similarities in



- 1110 ground- and satellite-based ndvi time series and their relationship to physiological activity of a Scots pine forest in Finland. *Remote Sensing of Environment* 93, 225–237., 10.1016/j.rse.2004.07.006, 2004.
- Wang A, Li, KY., and Lettenmaier DP.: Integration of the Variable Infiltration Capacity Model Soil hydrology scheme into the Community Land Model. *Climate and Dynamics*, 1115 <https://doi.org/10.1029/2007JD009246>, 2008.
- Wang, X., Piao, S., Ciais, P., Friedlingstein, P., Myneni, R.B., Cox, P., Heimann, M., Miller, J., Peng, S., Wang, T., Yang, H., and Chen, A.: A two-fold increase of carbon cycle sensitivity to tropical temperature variations. *Nature* **506**, 212–215 (2014). doi:10.1038/nature12915 pmid:24463514, 2014.
- 1120 Ward, J. D., Seely, M. K., and Lancaster, N.: On the antiquity of the Namib, *S. Afr. J. Sci.*, 79, 175–183, 1983.
- Wilhite, D.A., and Glantz, M.H.: Understanding the drought phenomenon: the role of definitions, *Water Int.*, 10 (3), pp. 111–120, <https://doi.org/10.1080/02508068508686328>, 1985.
- 1125 Woodward, FI., and Lomas, MR.: Vegetation-dynamics – simulating responses to climate Change. *Biological Reviews* 79, 643 – 670, <https://doi.org/10.1017/S1464793103006419>, 2004.
- WRI (World Resources Institute). 2000. World resources 2000–2001. People and ecosystems: Xu, K., Yang, D., Yang, H., Li, Z., Qin, Y., Shen, Y.: Spatio-temporal variation of drought 1130 in China during 1961–2012: a climatic perspective *J. Hydrol.*, 526, pp. 253–264, 10.1016/j.jhydrol.2014.09.047, 2015.
- Xue, J., and Su, B.: Significant remote sensing vegetation indices: a review of developments and applications, *J. Sens.*, p. 17, <https://doi.org/10.1155/2017/1353691>, 2017.
- Yang, Y, J., Fang, J., W, Ma and Wang, W.: Relationship between variability in aboveground 1135 Net primary production in global grasslands. *Geophy Res Lett* Vol 35, 123710, doi:10.1029/2008GLO35408, 2008.
- Yin, Y., Byrne, B., Liu, J., Wennberg, P., Davis, K. J., Magney, T., et al.: Cropland carbon uptake delayed and reduced by 2019 Midwest floods. *AGU Advances*, 1, e2019AV000140. <https://doi.org/10.1029/2019AV000140>., 2020.
- 1140 Zaehle, S., Ciais, P., Friend, A. D., and Prieur, V.: Carbon benefits of anthropogenic reactive nitrogen offset by nitrous oxide emissions, *Na. Geosci.*, 4, 601–605, <https://doi.org/10.1038/NGEO1207>, 2011.
- Zeppel MJB, Wilk JV and Lewis JD.: Impacts of extreme precipitation on plants. *Biogeosciences*, 11, 3083 – 3093. doi. 10.5194/bg-11 3083-2004, 2014.
- 1145 Zhang, L., Xiao, J., Li, J., Wang, K., Lei, L., and Guo, H.: The 2010 spring drought reduced primary productivity in southwestern China, *Environ. Res. Lett.*, 7 (4), p. 045706, 10.1088/1748-9326/7/4/045706, 2012
- Zhao, C., Deng, X., Yuan, Y., Yan, H., and Liang, H.: Prediction of drought risk based on the WRF model in yunnan province of China *Adv. Meteorol.*, pp. 1–9, 1150 <https://doi.org/10.1155/2013/295856>, 2013.